Title:

Different activation signals induce distinct mast cell degranulation strategies

Nicolas Gaudenzio[1,2], Riccardo Sibilano[1,2,#], Thomas Marichal[3,#], Philipp Starkl[1,2], Laurent L. Reber[1,2], Nicolas Cenac[4], Benjamin D. McNeil[5], Xinzhong Dong[5,6], Joseph D. Hernandez[1,2], Ronit Sagi-Eisenberg[7], Ilan Hammel[8], Axel Roers[9], Salvatore Valitutti[4], Mindy Tsai[1,2], Eric Espinosa[4,*] and Stephen J. Galli[1,2,10,*].

[1] Department of Pathology, Stanford University School of Medicine, Stanford, CA 94305, USA

[2] Sean N. Parker Center for Allergy Research, Stanford University School of Medicine, CA 94305, USA

[3] GIGA-Research and Faculty of Veterinary Medicine, University of Liege, Liege, Belgium

[4] Institut National de la Santé et de la Recherche Médicale, U1043, Toulouse F-31300, Inserm, U1043, Toulouse, France

[5] The Solomon H. Snyder Department of Neuroscience, Center for Sensory Biology Johns Hopkins University, School of Medicine, Baltimore, MD 21205

[6] Howard Hughes Medical Institute, Johns Hopkins University School of Medicine, Baltimore, MD 21205

[7] Department of Cell and Developmental Biology, Sackler Faculty of Medicine, Tel-Aviv University, Ramat Aviv, Tel Aviv, Israel 69978

[8] Department of Pathology, Sackler Faculty of Medicine, Tel-Aviv University, Ramat Aviv, Tel Aviv, Israel 69978

[9] Institute for Immunology, University of Technology Dresden, Medical Faculty Carl-Gustav Carus, 01307 Dresden, Germany

[10] Department of Microbiology & Immunology Stanford University School of Medicine, Stanford, CA 94305, USA

[#] and * Equal contribution; correspondence should be addressed to:

Eric Espinosa
UMR 1043 INSERM
CPTP CHU Purpan
BP3028
31024 Toulouse, France
Telephone: 0562748304
Email: eric.espinosa@inserm.fr (E.E.)
or
Stephen J. Galli
269 Campus Drive, Room 3255b
Stanford, CA 94305-5176, USA
Telephone: (650) 736-6014
Email: sgalli@Stanford.edu

Supplemental Methods

Mice.

C57BL/6J (WT) mice were obtained from Jackson Laboratories and either bred at the Stanford University Research Animal Facility or used for experiments after maintaining the mice for at least two weeks in our animal facility. C57BL/6-*Kit*$^{W\text{-}sh/W\text{-}sh}$ mice were originally provided by Peter Besmer (Molecular Biology Program, Memorial Sloan-Kettering Cancer Center, New York, NY, USA); we then backcrossed these mice to C57BL/6J mice for more than 11 generations(1). C57BL/6-*Mcpt5-Cre*$^{+}$ mice were provided by Axel Roers (Institute for Immunology, University of Technology Dresden, Medical Faculty Carl-Gustav Carus, Dresden, Germany) and bred at the Stanford University Research Animal Facility. B6.129X1-*Gt(ROSA)26Sor*$^{tm1(EYFP)Cos}$/J (*R26Y*$^{+}$) mice were obtained from Jackson Laboratories and bred at the Stanford University Research Animal Facility. C57BL/6-*MrgprB2*^{MUT} and C57BL/6-*MrgprB2*$^{+/+}$ littermate control mice were provided by Xinzhong Dong (The Solomon H. Snyder Department of Neuroscience, Johns Hopkins University, Baltimore, USA) and bred at the Stanford University Research Animal Facility. We used age-matched (8-10 weeks old) female mice for all experiments, except for experiments using *MrgprB2*^{MUT} and littermate controls where both age-matched male and female mice were used.

MC stimuli.

Substance P acetate (#S6883), compound 48/80 (#C2313), Endothelin-1 (#E7764), and 2, 4-dinitrophenyl-conjugated human serum albumin (DNP-HSA, #A6661) were all from Sigma Aldrich, USA. Icatiban HOE140 (#22968) and Cetrorelix acetate (#60869) were both from Anaspec, USA. Recombinant human complement component C5a (#2037-C5-025) was from R&D systems, USA, and recombinant human complement component C3a (#204881) was from Calbiochem, USA. Mouse anti-dinitrophenol (DNP) mAb was from Abnova (#MAB3977).

Immunoprecipitation and Western blot analysis.

3x 10^6 PBCMCs were used for each condition and tested at various time points. Human IgE-sensitized (2 μg/ml, for 16 hours) or non-sensitized PBCMCs were washed and stimulated with 2 μg/ml of anti-IgE or 10 μM SP respectively (**Figures 3, 4**). PBCMC lysates were prepared in 100 μl lysis buffer (#89856C, Thermo Scientific) supplemented with protease inhibitors (Roche) according to the manufacturer's instructions. PBCMCs were lysed at resting condition (0 minutes), and at 5 and 15 minutes after addition of stimuli. For Western blot analysis, total protein extracts were resolved onto a polyacrylamide gel, under reducing conditions. Blotted extracts were probed with the indicated antibodies. For immunoprecipitation experiments, lysates were mixed with Dynabeads Protein G Immunoprecipitation Kit resin (#10007D, Life Technologies) and proteins of interest were immunoprecipitated according to the manufacturer's instructions. Elution of the protein complexes was performed under non-reducing conditions. Immunoprecipitated proteins were resolved onto a polyacrylamide gel under reducing conditions, blotted and probed with the indicated antibodies. For verification of the specificity of the antibodies used for immunoprecipitation (**Supplemental Figure 10**), we tested their reactivity with 0.5 μg of the following recombinant proteins (all from Abcam): recombinant Human Syntaxin 3 protein (#ab124597), recombinant Human Syntaxin 4 protein (#ab114464), and recombinant Human SNAP23 protein (#ab79180).

Measurements of lipid mediators.

Supernatant lipid extraction.

To 500 µl of cell supernatant, we added 5 µl of internal standard (LxA4-d5, at 400 ng/ml, in MeOH) and 300 µl of cold methanol. Samples were centrifuged at 3000 rpm for 15 min at 4°C. Supernatants were collected, brought to a volume of 2 ml in H_2O and submitted to solid-phase extraction using HRX-50 mg 96-well (Macherey Nagel, Hoerd, France) as previously

described(2). Solvent was evaporated under nitrogen and samples were dissolved with MeOH and stored at -80 °C for liquid chromatography/tandem mass spectrometry measurements.

Targeted LC-MS/MS-based lipidomics of mast cell supernatants.

To simultaneously separate lipids of interest (PGE_2 and PGD_2) and 1 deuterated internal standards, LC-MS/MS analysis was performed on an ultra-high performance liquid chromatography system (UHPLC, Agilent LC1290 Infinity) coupled to Agilent 6460 triple quadrupole MS (Agilent Technologies) equipped with electro-spray ionization operating in negative mode(2). Reverse-phase UHPLC was performed using a ZorBAX SB-C18 column (Agilent Technologies) with a gradient elution. The mobile phases consisted of water, acetonitrile (ACN) and formic acid (FA) (75:25:0.1;v/v/v) (A) and ACN, FA (100:0.1, v/v) (B). The linear gradient was as follows: 0% B at 0 min, 85% B at 8.5 min, 100% B at 9.5 min, 100% B at 10.5 min and 0% B at 12 min. The flow rate was 0.35 ml/min. The autosampler was set at 5°C and the injection volume was 5 µl. Data were acquired in Multiple Reaction Monitoring (MRM) mode with optimized conditions. Peak detection, integration and quantitative analysis were done using Mass Hunter Quantitative analysis software (Agilent Technologies). For each standard, calibration curves were built using 10 solutions at concentration ranging from 0.95 ng/ml to 500 ng/ml. A linear regression with a weight factor of 1/X was applied for each compound. The limit of detection (LOD) and the limit of quantification (LOQ) were determined for the 2 compounds using signal to noise ratio (S/N). The LOD corresponded to the lowest concentration leading to a signal to noise over 3 and LOQ corresponded to the lowest concentration leading to a signal to noise over 10. All values under the LOQ were not considered. Importantly, blank samples were evaluated, and their injection showed no interference (no peak detected), during the analysis.

IgE-dependent systemic anaphylaxis and substance P-induced systemic responses.

IgE-dependent systemic anaphylaxis.

We used the passive systemic anaphylaxis (PSA) model to induce a systemic IgE-dependent reaction. Mice were sensitized by mean of intraperitoneal injection (i.p.) of 10 μg of mouse DNP-HSA-specific IgE(3, 4) in 200 μl PBS, and control mice were mock-injected i.p. with 200 μl of PBS. 16 hours later, sensitized or non-sensitized control mice were injected i.p. with 500 μg of DNP-HSA and rectal temperature was measured at different time points during a period of 120 min.

Substance P-induced systemic reactions.

Mice were injected i.p. with 200 μl of PBS in order to receive a treatment similar to that of the IgE-sensitized mice. 16 hours later, mice were injected i.p. with 1 mg of SP in 200 μl PBS or 200 μl PBS as a control, and rectal temperature was measured at different time points during a period of 120 min.

The doses of DNP-HSA and SP we used in these experiments were the doses which, in preliminary experiments, induced the strongest drop in body temperature.

IgE-dependent and substance P-dependent cutaneous inflammation.

The left and right ear pinnae of C57BL/6 wild type mice were sensitized by means of an intradermal (i.d.) injection with mouse DNP-HSA-specific IgE(5) (20 ng in 20 μl PBS) or received an i.d. injection of 20 μl PBS (control), respectively. 16 h later, the left ear pinna was injected i.d. with DNP-HSA (5 ng in 20 μl) to induce IgE-dependent inflammation, while the right ear pinna was injected i.d. with SP (1 nmol in 20 μl) to induce IgE-independent inflammation. Some ear pinnae were injected i.d. with 20 μl of PBS to assess the extent to which the observed inflammation was due to the i.d. injection. Measurement of Evan's blue dye extravasation and ear swelling, and toluidine blue and hematoxylin and eosin staining (H&E) of histological sections of ear pinnae, were performed as previously described(5).

Foot pad challenge and assessment of effects on draining lymph nodes (DLNs).

The left and right foot pads of C57BL/6 wild type mice were sensitized by means of an intradermal (i.d.) injection with mouse DNP-HSA-specific IgE(5) (20 ng in 20 μl PBS) or 20 μl PBS (control), respectively. 16 h later, the left foot pad was injected i.d. with DNP-HSA (5 ng in 20 μl) to induce IgE-dependent inflammation, while the right foot pad was injected i.d. with SP (1 nmol in 20 μl) to induce IgE-independent inflammation. Some foot pads were injected i.d. with 20 μl of PBS to assess the extent to which the observed inflammation was due to the i.d. injection. Measurement of Evan's blue dye extravasation and toluidine blue staining of foot pad histological sections were performed as previously described(5). In some experiments, histological sections of DLNs were stained with toluidine blue or Av.SRho 2 hours after challenge to assess whether LN-resident MCs exhibited degranulation and to search for the presence of mast cell granule structures(6). The presence of individual metachromatic granule structures in DLNs was carefully assessed by light microscopy using an X100 oil objective on Toluidine Blue-stained sections, whereas we examined sections of the DLNs for the presence of Av.SRho$^+$ mast cell granule structures by immunofluorescence. In other experiments, DLNs were removed and weighed 24 hours after injection of the footpads(6).

Peripheral blood mononuclear cell-derived human mast cells.

Peripheral blood mononuclear cells were obtained from buffy coats of healthy blood donors at the Stanford Blood Center. CD34$^+$ precursor cells were isolated from peripheral blood mononuclear cells (EasySep Human CD34 Positive Selection Kit, STEMCELL Technologies). CD34$^+$ cells were maintained for 1 week under serum-free conditions using StemSpan medium (STEMCELL Technologies) supplemented with recombinant human IL-6 (50 ng/ml; Peprotech), human IL-3 (10 ng/ml; Peprotech) and 3% supernatant of CHO transfectants secreting murine SCF (a gift from Dr P. Dubreuil, Marseille, France, 3% correspond to ~50 ng/ml SCF). Thereafter, the cells

were maintained in IMDM Glutamax I, sodium pyruvate, 2-mercaptoethanol, 0.5% BSA, insulin-transferrin selenium (all from Invitrogen), ciprofloxacin (10 μg/ml; Sigma-Aldrich), IL-6 (50 ng/ml) and 3% supernatant of CHO transfectants secreting mouse SCF. Before use in experiments, PBCMCs were tested for phenotype by flow cytometry (tryptase, chymase, CD117, FcεRI) and function (β-hexosaminidase release in response to FcεRI cross-linking) at 8-12 weeks. PBCMCs were usually ready for experiments after ~10 weeks in culture.

Generation and culture of mouse peritoneal cell-derived mast cells (PCMCs).

PCMCs were generated as previously described(7, 8). Briefly, Peritoneal cells from C57BL/6 mice were collected and seeded in Opti-MEM medium supplemented with 10% FCS, 100 IU/mL penicillin, 100 µg/mL streptomycin (Invitrogen), and 3% supernatant of CHO transfectants secreting mouse SCF (a gift from Dr. P. Dubreuil, Marseille, France). 24 hours later, nonadherent cells were removed and fresh culture medium was added to adherent cells. Three days later, nonadherent cells and adherent cells were harvested by flushing and resuspended in fresh culture medium. The same procedure was repeated twice a week. Cells were used for experiments between weeks 4 and 10, when MCs represented >95%% of the cell population(8).

Antibodies.

Rabbit polyclonal IgG anti-phospho IKKα (Ser176)/IKKβ (Ser177) (C84E11), PKC (gamma T514), AKT (T308) and rabbit polyclonal IgG anti-actin antibodies were from Cell Signaling Technology, USA. Rabbit polyclonal IgG anti-SNAP-23 (Ab4114) and anti-Syntaxin 4 (STX-4, Ab101879) and rabbit polyclonal IgG anti-Syntaxin 3 (STX-3, Ab4113) were from Abcam, USA. Rabbit polyclonal IgG anti-Munc 18-2 was from Proteintech, USA. Rat IgG2b-APC isotype control (clone eB149/10H5), Rat IgG2b-FITC isotype control (clone eB149/10H5), Rat IgG2a-PE isotype control (clone r2a-21B2), rat IgG2b anti-mouse CD45-APC (clone 30-F11) and rat IgG2b anti-mouse GR-

1-FITC (clone RB6-8C5) were all from eBioscience, USA. Rat IgG2a anti-mouse F4/80-PE (clone BM8) was from Biolegend, USA, human IgE myeloma was from Calbiochem, USA, and rabbit anti-human IgE were from Bethyl Laboratories, USA. Mouse IgG2a anti-human IgE (clone MH25-1) and goat polyclonal IgG anti-human tryptase (G-12) were both from Santa Cruz Biotechnology, USA. Mouse IgG1 anti-DNP (clone B136M) was from Abnova, Taiwan. Mouse IgE anti-DNP clone ε26(9) was initially provided by Dr. Fu-Tong Liu, University of California–Davis, Davis, CA, USA.

MRGPRX2 knock down by shRNA transfection.

E. coli-amplified Suresilencing shRNA plasmids from Qiagen were used. PBCMCs were generated as described in the main Methods section. After 10 weeks of culture, $1x10^6$ PBCMCs were transfected using the Attractene reagent (Qiagen) with 1.2 µg DNA of *MRGPRX2* Suresilencing shRNA plasmids (Qiagen, Cat# KM59132G) or negative control shRNA plasmids both containing a reporter GFP in 6-well plates, for 48 hours. The degranulation dynamics of GFP-expressing PBCMCs were analyzed by confocal laser-scanning microscopy (as described below).

Measurement of secretion of mast cell mediators and cytokines in vitro.

$1x10^5$ IgE-sensitized (1 µg/ml for 16 hours) or non-sensitized PBCMCs were plated in 100 µl of IMDM with GlutaMAX-I, sodium pyruvate, 2-mercaptoethanol, 0.5% BSA and 0.5% supernatant of Chinese hamster ovary transfectants secreting mouse stem cell factor. Different concentrations of anti-human IgE or SP were added to IgE-sensitized and non-sensitized PBCMCs, respectively, for different periods of time and the amount of MC degranulation was assessed as % release of total β-hexosaminidase(10) the amounts of lipid mediators release were quantified as described above in ***Measurements of lipid mediators***, and the amounts of secreted cytokines were quantified in the supernatants by cytometric bead array (CBA, BD Bioscience, USA) according to the manufacturer's recommendations.

IKKβ inhibition in MCs.

$2x10^6$ PBCMCs were incubated for 60 min at 37°C with 100 μM of BMS-345541 (4[2'-aminoethyl]amino-1,8-dimethylimidazo[1,2-a]quinoxaline, Sigma Aldrich) in dimethyl sulfoxide (DMSO), or with the same volume of DMSO alone, before performing the experiments described in **Figure 4**.

Flow cytometry analyses.

Mast cell degranulation analysis.

$5x10^4$ human IgE-sensitized or non-sensitized PBCMCs were plated in 100 μl of Tyrode's buffer and stimulants were added to the cell culture. 30 to 60 min later, 5 μg/ml of Alexa488-coupled avidin (Av.A488, #A-21370, Life Technologies, USA) was added together with 1 μg/ml of propidium iodide (PI, to assess cell viability, #P3566, Life Technologies, USA) and PI^- $Av.A488^+$ PBCMCs were analyzed using an AccuriC6 flow cytometer (BD Bioscience, USA). For time-lapse flow cytometry analyses, $5x10^5$ IgE-sensitized or non-sensitized PBCMCs were stimulated as previously described in a final volume of 1 ml Tyrode's buffer supplemented with 5μg/ml of Av.A488. Detection of PI^- $Av.A488^+$ PBCMCs was recorded upon addition of stimulatory molecules using the time-lapse function of an AccuriC6 flow cytometer (BD Bioscience, USA).

Analysis of tissue immune cells.

One cm^2 ear pinnae sections were cut into small pieces and digested in Dulbecco's Modified Eagle's medium (DMEM) supplemented with 20 mM HEPES, 10 μg/ml of Collagenase, Hyaluronidase and DNAse for 90 min at 37 °C while shaking. Tissue suspensions were then filtered and cells were stained with primary antibodies directed against different immune cells populations (neutrophils, monocytes/macrophages and T lymphocytes). One μg/ml of PI were

added to the cell suspensions and PI^- $CD45^+$ immune cell populations were analyzed using a flow cytometer AccuriC6 (BD Bioscience).

Transmission Electron Microscopy.

PBCMCs were pelleted and re-suspended in 10% Gelatin in 0.1M Sodium Cacodylate buffer pH = 7.4 at 37ºC and allowed to equilibrate for 5 minutes. Cells were pelleted again, excess gelatin was removed, and the cells then were chilled in cold blocks, covered with cold 1% Osmium tetroxide (EMS Cat# 19100), and rotated for 2 hours in a cold room. The fixed specimens then were washed 3X with cold ultrafiltered water, then stained overnight in bloc in 1% Uranyl Acetate at 4ºC while rotating. Samples were then dehydrated in a series of ethanol washes for 20 minutes each at 4ºC beginning at 30%, 50%, 70%, and 95%, when the samples then were allowed to rise to RT, changed to 100% ethanol 2X, then Propylene Oxide (PO) for 15 min. Samples were infiltrated with EMbed-812 resin (EMS Cat#14120) mixed 1:2, 1:1, and 2:1 with PO for 2 hours each, then samples were left in 2:1 resin:PO overnight rotating at RT in the hood. The samples were then placed into EMbed-812 for 2 to 4 hours, then placed into molds with labels and fresh resin, orientated, and placed into a 65º C oven overnight. Sections were taken at ~ 80nm, picked up on formvar/Carbon-coated 100 mesh Cu grids, stained for 30 seconds in 3.5% Uranyl Acetate in 50% Acetone followed by staining in 0.2% Lead Citrate for 3 minutes. Sections were examined in a JEOL JEM-1400 120kV and photos were taken using a Gatan Orius 4k X 4k digital camera. Images of 30 intact mast cells in photomicrographs from each specimen analyzed were selected randomly (by taking pictures of mast cells in sequence as they appeared in the microscope field), and, for each mast cell, the area of the section of each exteriorized granule structure which appeared to be separated from the cell was analyzed using area function of ImageJ software. For each experimental condition analyzed, 700 to 750 exteriorized granule structures were measured.

Confocal laser-scanning microscopy.

Single cell analysis of mast cell degranulation dynamics.

$5x10^4$ human IgE-sensitized or non-sensitized PBCMCs were placed into poly-D-Lysine-coated (5 μg/ml in water, #P6407, Sigma Aldrich, USA) Nunc Lab-Tek 1.0 borosilicate cover glass system 8 chambers (#155411, Thermoscientific, USA) in Tyrode's buffer supplemented with 5 μg/ml of avidine-sulforodamine 101 (Av.SRho, #A2348, Sigma Aldrich, USA), as previously described(11). Stimuli were added and fluorescence was recorded each 2.3 seconds in a controlled atmosphere (using a Zeiss stage-top incubation system with objective heater, 37°C and 5% humidified CO_2) using a Zeiss LSM710 or a Zeiss LSM780 Meta inverted confocal laser-scanning microscope, 20x/0.8 WD=0.55 M27 objective and electronic zoom 1 (8 bits/pixel 512x512) for single cell Av.SRho fluorescence monitoring, and 63x/1.40 Oil DIC M27 objective and electronic zoom 3 (dimension x:512 y:512, scaling x= 0.264 μm and y= 0.264 μm) for high resolution single cell analyzes or monitoring of individual granule structures. In some experiments, cells were also loaded with 1 μg Fluo-4 AM (#F-14217, Life Technologies, USA) to monitor $[Ca^{2+}]i$ levels, and data were presented as fold-increase from Fluo-4 fluorescence measured before addition of any stimulus. Mean fluorescence intensity (MFI) was quantified using the Measurement function of Image J software, on randomly selected fields and untreated image sequences. Modeling and analysis of budding granule structures were performed on untreated image sequences, as described below in the "**Granule modeling and analysis**" section.

Dextran-FITC dequenching assay.

$5x10^4$ PBCMCs were incubated with 1 mg/ml fluorescein isothiocyanate-dextran (dextran-FITC, #46945, Sigma Aldrich, USA) for 48 hours in previously described culture medium(12). $5x10^4$ dextran-FITC-loaded human IgE-sensitized or non-sensitized PBCMCs were placed into poly-D-Lysine-coated Nunc Lab-Tek 1.0 borosilicate cover glass system 8 chambers in Tyrode's buffer supplemented with 5 μg/ml of Av.SRho, as described above. Stimuli were added and dextran-

FITC and Av.SRho fluorescence signals were recorded simultaneously in a controlled atmosphere. To avoid any bleaching of FITC fluorescence due to repeated laser exposures, images were acquired every 10 seconds using a Zeiss LSM780 Meta inverted confocal laser-scanning microscope, 20x/0.8 WD=0.55 M27 objective and electronic zoom 1 (8 bits/pixel 256x256). MFI was quantified on randomly selected fields and untreated image sequences using the Measurement function of Image J software. To correct for differences in the loading of dextran-FITC between PBCMCs and experiments, the dextran-FITC fluorescence of each single unstimulated PBCMC was normalized to reach the average of dextran-FITC fluorescence per cell measured over all the experiments.

In vitro 3-D degranulation assay.

$5x10^3$ Fluo-4-loaded human IgE-sensitized or non-sensitized PBCMCs were embedded in 200 μl of a 7.8 mg/ml Matrigel Matrix (#354248, Corning, USA) and placed in Nunc Lab-Tek 1.0 borosilicate cover glass system 8 chambers in Tyrode's buffer supplemented with 5 μg/ml of Av.SRho, as described above. 30 min after stimuli addition, z-stack images sequence corresponding to randomly selected single PBCMCs were acquired in 3-D up to 20-30 μm depth, with 20x/0.8 WD=0.55 M27 objective and electronic zoom 3 (8 bits/pixel 512x512, scaling x= 0.277 μm, y= 0.277 μm, z= 1.0 μm). Modeling and analysis of released granule structures were performed on untreated image sequences, as described below in the "**Granule modeling and analysis**" section.

Two-photon microscopy.

Single cell analysis of tissue mast cell granule characteristics.

The ear pinnae of C57BL/6-*Mcpt5-Cre*$^+$; *R26Y*$^+$ mice were sensitized by i.d. injection of 20 ng of mouse anti-DNP IgE(5) in 20 μl PBS or received an i.d. injection of 20 μl PBS as a control. 16 h later, 8 μg of Av.SRho in 20 μl were injected i.d. into the ear pinna under the two-photon

microscope, anesthesia was maintained by a mixture of Isoflurane/O_2 and the animal's ear pinna was kept at 36°C using a heating pad system for 20 min. To induce a SP-mediated systemic anaphylaxis, non-sensitized *Mcpt5-Cre*$^+$; *R26Y*$^+$ mice received an i.p. injection of 1 mg of SP in 200 μl of PBS. To induce IgE-mediated systemic anaphylaxis, anti-DNP IgE-sensitized *Mcpt5-Cre*$^+$; *R26Y*$^+$ mice received an i.p. injection of 500 μg of DNP-HSA in 200 μl PBS. Control mice received an i.p. injection of 200 μl PBS. 30 to 60 min later, the fluorescence corresponding to Av.SRho$^+$ granule structures surrounding EYFP$^+$ dermal MCs was measured using a Prairie Ultima IV two-photon microscope (Spectra Physics Mai Tai HP Ti:sapphire laser, tunable from 690 to 1040 nm). Images were acquired in 3-D up to 30-50 μm depth, with 20x Olympus XLUM Plan Fl N.A. 0.95 water-immersion objective and a software zoom setting of 3 (8 bits/pixel 1024x1024, scaling x= 0.228 μm, y= 0.228 μm, z= 0.5 μm). Modeling and analysis of released granule structures were performed using untreated image sequences, as described below in the "**Granule modeling and analysis**" section.

Intravital analysis of vascular permeability.

The ear pinnae of C57BL/6 wild type mice were sensitized by i.d. injection of 20 ng of mouse anti-DNP IgE(5) in 20 μl PBS or just received an i.d. injection of 20 μl PBS as a control. 16 hours later, mice were positioned under the two-photon microscope, anesthesia was maintained by a mixture of Isoflurane/O_2 and the animal's ear pinna was kept at 36°C using a heating pad system for 20 min. To visualize the flowing blood, mice received a retro-orbital injection of 5 mg of 70-kDa dextran-FITC (#46945, Sigma Aldrich, USA) in 200 μl of PBS, as previously reported(13). To induce a SP-mediated systemic response, non-sensitized *Mcpt5-Cre*$^+$; *R26Y*$^+$ mice received an i.p. injection of 1 mg of SP in 200 μl PBS. To induce IgE-mediated systemic anaphylaxis, anti-DNP IgE-sensitized *Mcpt5-Cre*$^+$; *R26Y*$^+$ mice received an i.p. injection of 500 μg of DNP-HSA in 200 μl PBS. Control mice received an i.p. injection of 200 μl PBS. Directly after injection of stimulus or PBS, the fluorescence corresponding to dextran-FITC-label in the blood stream was

recorded using the same two photon microscope as described above. Images were acquired in 3-D up to 50-60 μm depth, with one 3-D images sequence per 1.52 min for 30 min, with 20x Olympus XLUM Plan Fl W. N/A95 w.d2.0 objective and electronic zoom 1 (8 bits/pixel 512x512, scaling x= 1.37 μm, y= 1.37 μm, z= 4 μm). The interstitial spaces were randomly circumscribed and changes in dextran-FITC MFI were measured(13). Data were presented as fold increase from basal MFI at t=0 on untreated image sequences using the Measurement function of Image J software version Fiji.

Granule modeling and analysis.

Granule modeling and measurement.

Untreated image sequences were processed using the Isosurface function of the Imaris Bitplane X64 software version 7.6.5 (Bitplane). Based on the detection of Av.SRho fluorescence intensity and employing precise measurements of the shape of the fluorescence signals, this software creates an artificial solid replica in 3-D of exteriorized Av.SRho$^+$ MC granule structures. The minimum estimated detectable surface was defined to be of 0.25 μm of diameter, in accord with the maximum resolution for 1 pixel obtained by each association microscope/objective/dimensions during the fluorescence acquisition process. For the LSM 710 or 780/63x/1.40 Oil DIC M27 objective scaling x= 0.264 μm and y= 0.264 μm, for the LSM 780/20x/0.8 WD=0.55 M27 scaling x= 0.277 μm, y= 0.277 μm and for the Prairie Ultima 4/20x Olympus XLUM Plan Fl W. N/A95 w.d2.0 objective scaling x= 0.228 μm, y= 0.228 μm. For each single cell inspected, individual modeled secretory granules were analyzed for their modeled volume and sphericity index. The same software settings were applied for all untreated images, to fairly analyze and compare each of the experimental conditions.

Virtual isolation of released granule.

In some experiments, we isolated and analyzed individual released structures, separately from the granule content that was attached to the cell surface. The body of each single MC was modeled based the fluorescence of Fluo-4 (for confocal microscopy) or of EYFP (for two photon microscopy) using the Isosurface function of the software. Data type was converted from 8 bits to 32 bits float, a step required by the software to initiate any Isosurface distance calculation. Av.SRho$^+$ granule structures were then modeled as described above and using the Distance Transformation function, Av.SRho$^+$ Isosurfaces (modeled externalized granule structures) were isolated from the Fluo-4/EYFP$^+$ Isosurface (modeled MC body) based on their proximity. Av.SRho$^+$ Isosurfaces overlapping with the Fluo-4/EYFP$^+$ Isosurface were systematically excluded from the analysis, as they correspond to the granule structures attached to the cell surface. In some experiments, isolated individual released granule structures were colored automatically according to their modeled volume or sphericity index, for a better appreciation of their different physical characteristics.

Supplemental References

1. Piliponsky, A.M., Chen, C.C., Grimbaldeston, M.A., Burns-Guydish, S.M., Hardy, J., Kalesnikoff, J., Contag, C.H., Tsai, M., and Galli, S.J. 2010. Mast cell-derived TNF can exacerbate mortality during severe bacterial infections in *C57BL/6-Kit*$^{W\text{-}sh/W\text{-}sh}$ mice. *Am J Pathol* 176:926-938.
2. Le Faouder, P., Baillif, V., Spreadbury, I., Motta, J.P., Rousset, P., Chene, G., Guigne, C., Terce, F., Vanner, S., Vergnolle, N., et al. 2013. LC-MS/MS method for rapid and concomitant quantification of pro-inflammatory and pro-resolving polyunsaturated fatty acid metabolites. *J Chromatogr B Analyt Technol Biomed Life Sci* 932:123-133.
3. Metz, M., Schafer, B., Tsai, M., Maurer, M., and Galli, S.J. Evidence that the endothelin A receptor can enhance IgE-dependent anaphylaxis in mice. *J Allergy Clin Immunol* 128:424-426 e421.
4. Lilla, J.N., Chen, C.C., Mukai, K., BenBarak, M.J., Franco, C.B., Kalesnikoff, J., Yu, M., Tsai, M., Piliponsky, A.M., and Galli, S.J. 2011. Reduced mast cell and basophil numbers and function in *Cpa3-Cre; Mcl-1*$^{fl/fl}$ mice. *Blood* 118:6930-6938.
5. Schafer, B., Piliponsky, A.M., Oka, T., Song, C.H., Gerard, N.P., Gerard, C., Tsai, M., Kalesnikoff, J., and Galli, S.J. 2012. Mast cell anaphylatoxin receptor expression can enhance IgE-dependent skin inflammation in mice. *J Allergy Clin Immunol* 131:m541-548.
6. Kunder, C.A., St John, A.L., Li, G., Leong, K.W., Berwin, B., Staats, H.F., and Abraham, S.N. 2009. Mast cell-derived particles deliver peripheral signals to remote lymph nodes. *J Exp Med* 206:2455-2467.
7. Malbec, O., Roget, K., Schiffer, C., Iannascoli, B., Dumas, A.R., Arock, M., and Daeron, M. 2007. Peritoneal cell-derived mast cells: an in vitro model of mature serosal-type mouse mast cells. *J Immunol* 178:6465-6475.

8. Gaudenzio, N., Espagnolle, N., Mars, L.T., Liblau, R., Valitutti, S., and Espinosa, E. 2009. Cell-cell cooperation at the T helper cell/mast cell immunological synapse. *Blood* 114:4979-4988.

9. Liu, F.T., Bohn, J.W., Ferry, E.L., Yamamoto, H., Molinaro, C.A., Sherman, L.A., Klinman, N.R., and Katz, D.H. 1980. Monoclonal dinitrophenyl-specific murine IgE antibody: preparation, isolation, and characterization. *J Immunol* 124:2728-2737.

10. Akahoshi, M., Song, C.H., Piliponsky, A.M., Metz, M., Guzzetta, A., Abrink, M., Schlenner, S.M., Feyerabend, T.B., Rodewald, H.R., Pejler, G., et al. 2011. Mast cell chymase reduces the toxicity of Gila monster venom, scorpion venom, and vasoactive intestinal polypeptide in mice. *J Clin Invest* 121:4180-4191.

11. Joulia, R., Gaudenzio, N., Rodrigues, M., Lopez, J., Blanchard, N., Valitutti, S., and Espinosa, E. 2015. Mast cells form antibody-dependent degranulatory synapse for dedicated secretion and defence. *Nat Commun* 6:6174.

12. Wollman, R., and Meyer, T. 2012. Coordinated oscillations in cortical actin and Ca(2+) correlate with cycles of vesicle secretion. *Nat Cell Biol* 14:1261-1269.

13. Egawa, G., Nakamizo, S., Natsuaki, Y., Doi, H., Miyachi, Y., and Kabashima, K. 2013. Intravital analysis of vascular permeability in mice using two-photon microscopy. *Sci Rep* 3:1932.

Supplemental Figures and Legends

Supplemental Figure 1

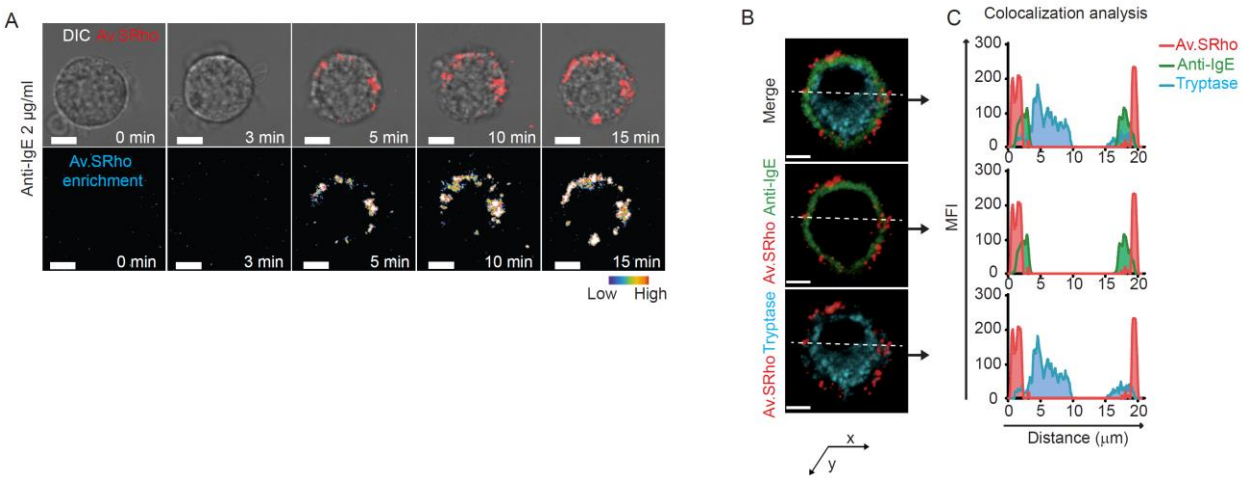

Supplemental Figure 1. Fluorochrome-labelled avidin enables real-time detection of exteriorized mast cell secretory granule structures. IgE-sensitized or non-sensitized PBCMCs were stimulated with 2 µg/ml of anti-IgE in the presence of Sulforhodamine 101-coupled avidin (Av.SRho, red). (**A**) Representative time-lapse sequence of a single PBCMC stimulated with anti-IgE; upper panel: Av.SRho fluorescence merged with Differential Interference Contrast (DIC), lower panel: Av.SRho enrichment (pseudocolor scale). (**B**, **C**) 30 min after degranulation, cells were fixed then stained with an Alexa488-coupled anti-IgE (green, to detect surface IgE), cells were then permeabilized and stained for tryptase content (blue). (**B**) Representative confocal microscopy pictures of a single degranulated PBCMC, Av.SRho, IgE and tryptase fluorescence are merged (upper panel), Av.SRho and IgE fluorescence are merged (mid panel), Av.SRho and tryptase fluorescence are merged (lower panel). (**C**) Fluorescence colocalization analysis for each of the pictures depicted in (**B**) along the white dotted line. Bar = 5µm.

Supplemental Figure 2

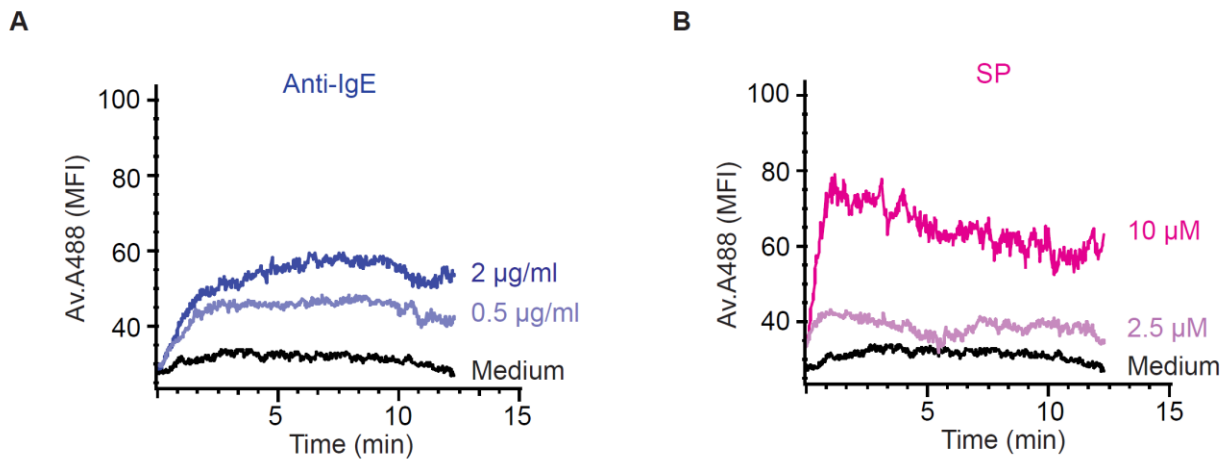

Supplemental Figure 2. Substance P- or anti-IgE-mediated mast cell degranulation dynamics does not depend on the concentration of stimulus. IgE-sensitized or non-sensitized PBCMCs were stimulated with 0.5 or 2 µg/ml of anti-IgE (blue) or with 2.5 or 10 µM of SP (pink), respectively, in the presence of Alexa488-coupled avidin (Av.A488). Fluorescence signal was measured using time-lapse flow cytometry. (**A**, **B**) Representative curves of Av.488 fluorescence signal monitoring in PBCMCs stimulated with (**A**) anti-IgE or (**B**) SP. Data are representative of the 3 independent experiments performed, each with PBCMCs from a different donor, each of which gave similar results.

Supplemental Figure 3

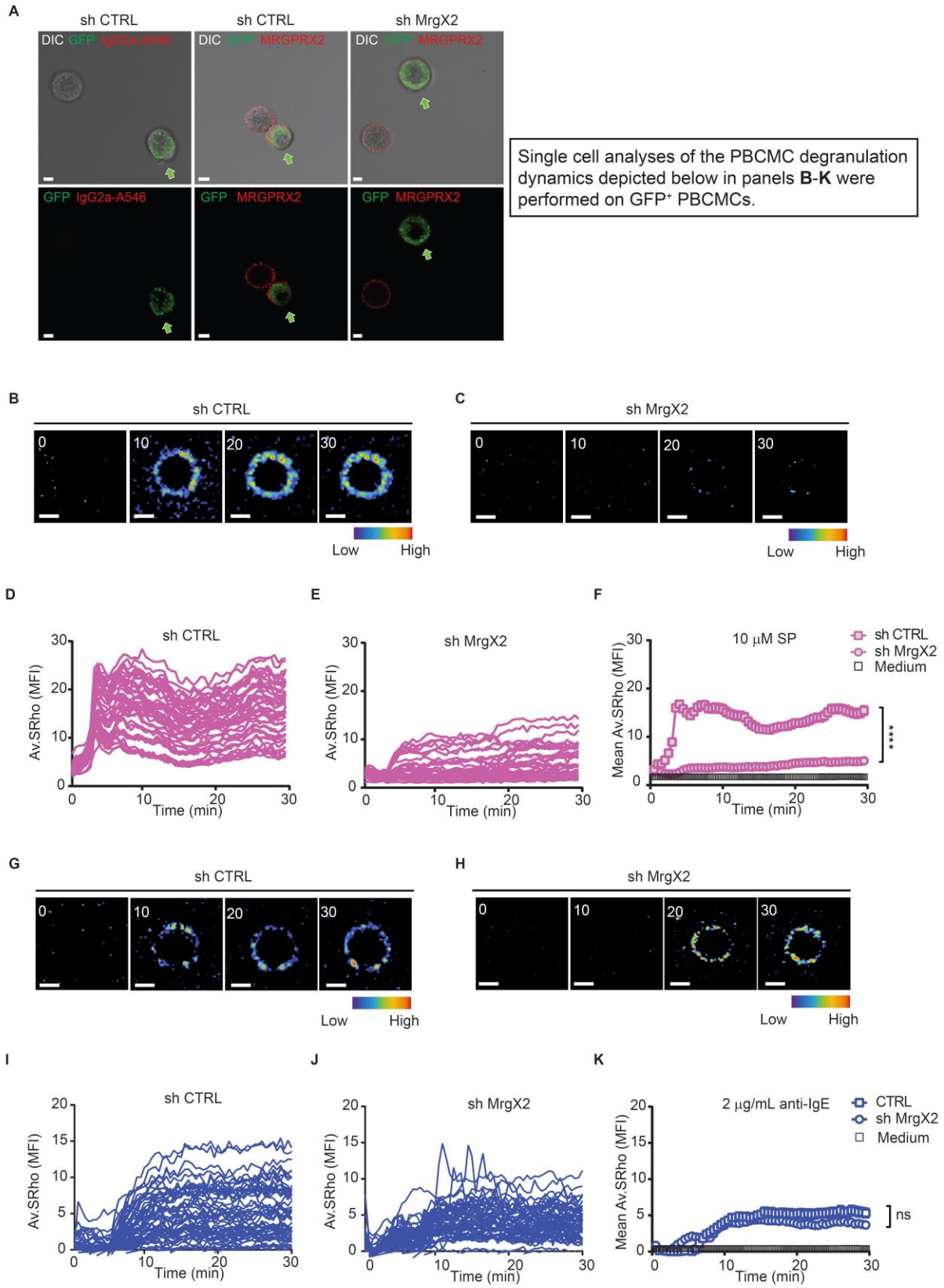

468

Supplemental Figure 3. In human mast cells, SP-induced rapid degranulation dynamics is mediated *via* MRGPRX2 activation. PBCMCs were transfected with shRNA control (shCTRL) or shRNA directed against *MRGPRX2* (shMrgX2). Each shRNA also encoded GFP to permit identification of the transfected cells. IgE-sensitized or non-sensitized previously transfected PBCMCs were stimulated or not with anti-IgE or SP, respectively, in the presence of Av.SRho. Av.SRho fluorescence was measured in single GFP^+ cells using time-lapse confocal microscopy in a controlled atmosphere (37°C and 5% CO_2). (**A**) Representative confocal microscopy pictures of MRGPRX2 (red) and GFP (green) staining in PBCMCs. Green arrows indicate shRNA-transfected PBCMCs expressing GFP. (**B**, **C**) Representative time-lapse sequence of Av.SRho enrichment (color scale) in a single (**B**) shCTRL-transfected PBCMC or (**C**) shMrgX2-transfected PBCMC stimulated with 10 μM of SP. Numbers = minutes (min). (**D**, **E**) Single cell analysis of Av.SRho MFI over time in individual (**D**) shCTRL-transfected PBCMCs or (**E**) shMrgX2-transfected PBCMC stimulated with 10 μM of SP or medium. (**F**) Mean curves of Av.SRho MFI in shCTRL- (pink squares) or shMrgX2- (pink circles) transfected PBCMCs stimulated with 10 μM of SP or medium (open squares). (**G**, **H**) Representative time-lapse sequence of Av.SRho enrichment (color scale) in a single (**G**) shCTRL-transfected PBCMC or (**H**) shMrgX2-transfected PBCMC stimulated with 2 μg/ml of anti-IgE. Numbers = minutes (min). (**I**, **J**) Single cell analysis of Av.SRho MFI in a single IgE-sensitized (**I**) shCTRL-transfected PBCMC or (**J**) shMrgX2-transfected PBCMC stimulated with 2 μg/ml of anti-IgE or medium. (**K**) Mean curves of Av.SRho MFI in IgE-sensitized shCTRL- (blue squares) or shMrgX2- (blue circles) transfected PBCMCs stimulated with anti-IgE or medium (open squares). Bars = 5 μm. Two-way ANOVA, ****P<.0001. Data are pooled from the 3 independent experiments performed with PBCMCs from one donor (25 single PBCMCs analyzed per condition), each of which gave similar results.

Supplemental Figure 4

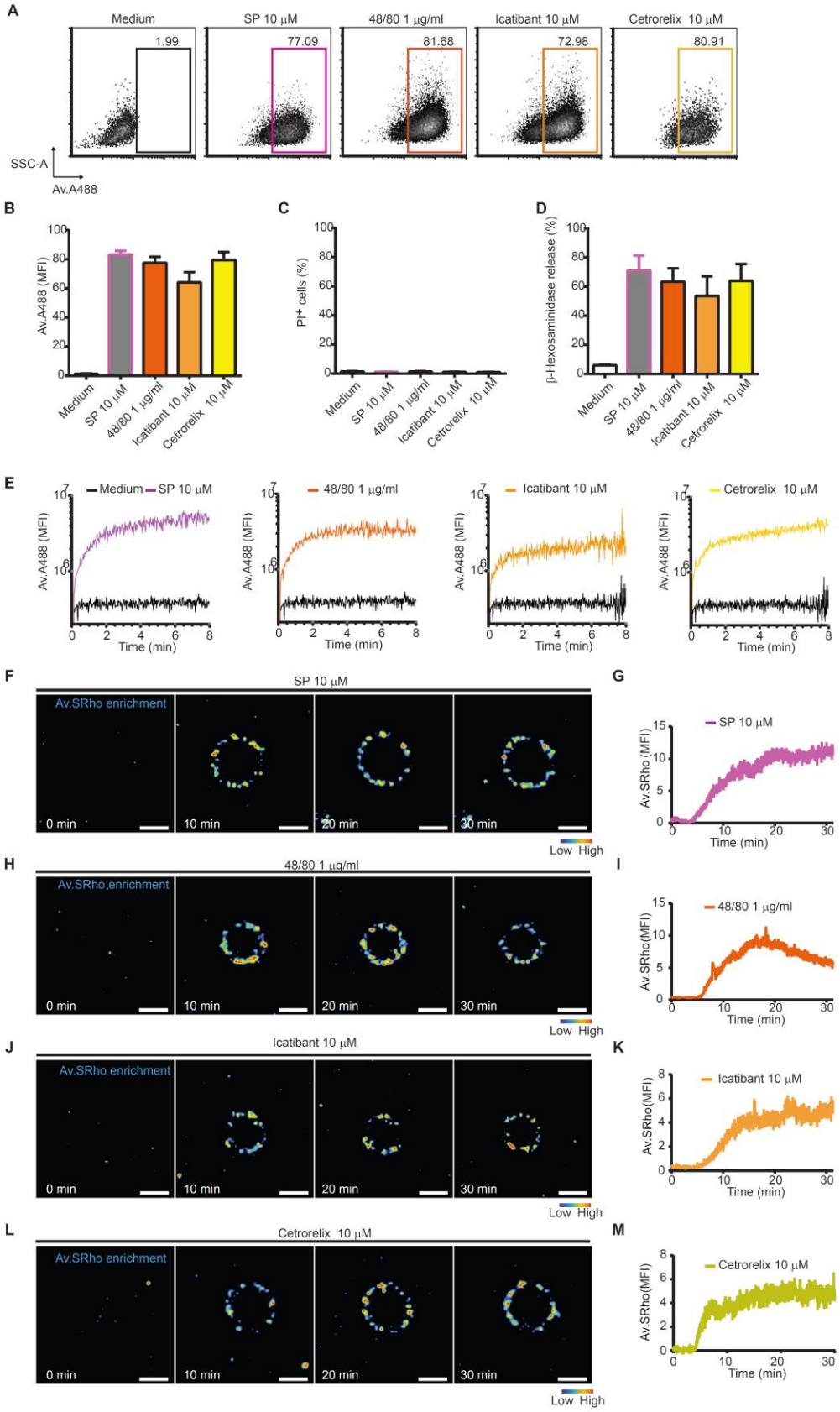

492

Supplemental Figure 4. Human mast cell activation by different cationic ligands results in similar degranulation dynamics. Non-sensitized PBCMCs were stimulated with 10 μM of SP (pink), 1 μg/ml of compound 48/80 (brown), 10 μM of Icatibant (orange) or 10 μM of Cetrorelix (yellow) in the presence of Av.A488 (for flow cytometry) or Av.SRho (for confocal microscopy). (**A**) Representative flow cytometry dot plots of Av.A488 fluorescence in PBCMCs 30 min after addition of cationic stimuli or medium. (**B**) Av.A488 fluorescence intensity, (**C**) propidium Iodide (PI) staining, and (**D**) percentage of β-hexosaminidase release in PBCMCs 30 min after addition of cationic stimuli or medium. Mean + SEM; data are pooled from the 3 independent experiments performed with PBCMCs from 3 different donors, each of which gave similar results. (**E**) Representative curves of Av.488 fluorescence signal monitoring in PBCMCs upon addition of cationic stimuli or medium. (**F**) Representative time-lapse sequence of Av.SRho enrichment (color scale) in a single PBCMC stimulated with 10 μM of SP. (**G**) Analysis of Av.SRho MFI in the PBCMC depicted in (**F**). (**H**-**M**) Same experiments as in (**F**, **G**) but with, respectively, (**H**, **I**) 1 μg/ml of compound 48/80, (**J**, **K**) 10 μM of Icatibant, or (**L**, **M**) and 10 μM of Cetrorelix. Bars = 5 μm. Data are representative of 10 single cells analyzed for each condition of stimulation with PBCMCs from 3 different donors, with replicate experiments giving similar results.

Supplemental Figure 5

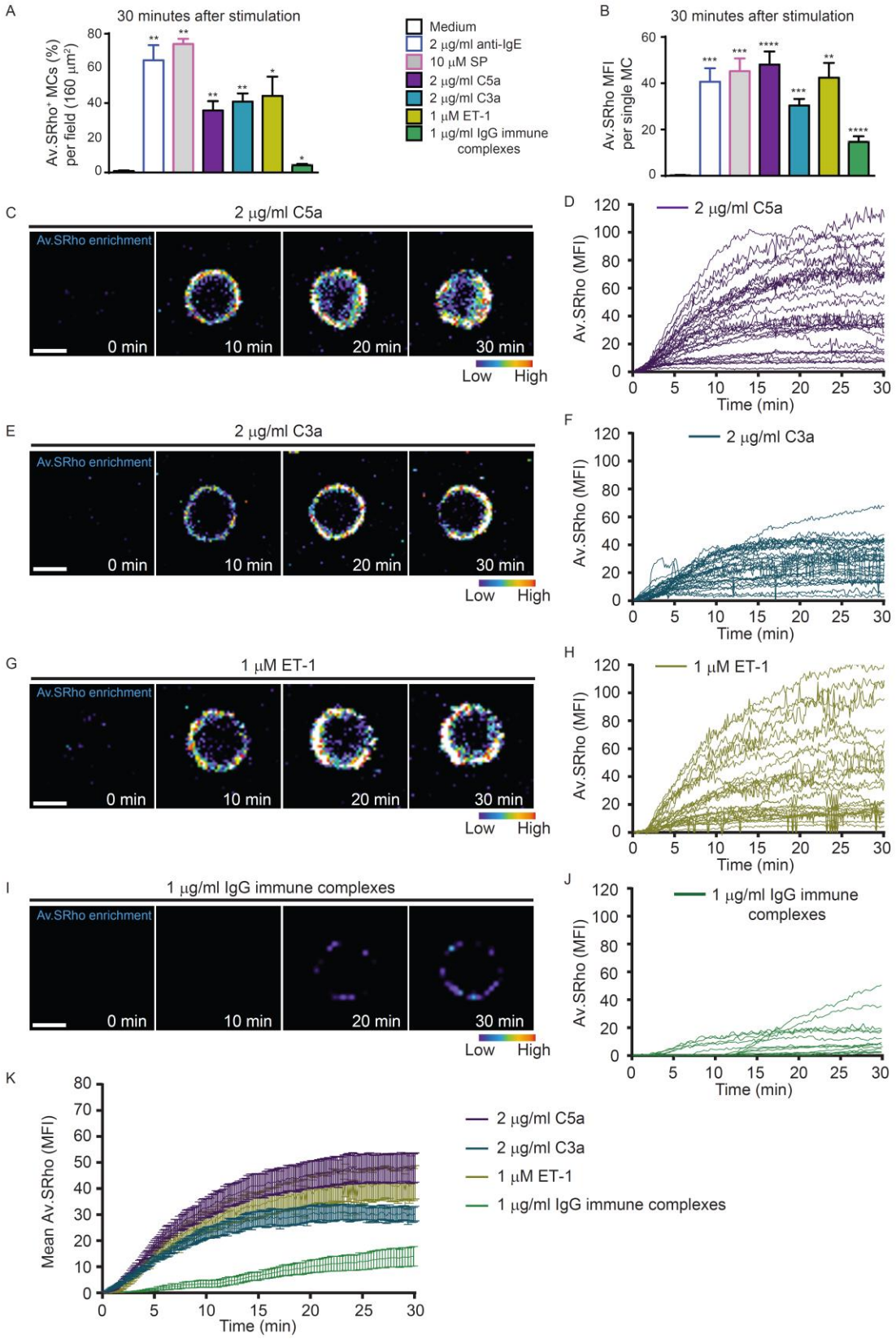

509

Supplemental Figure 5. Human mast cell activation by C3a, C5a or ET-1 induces a spatio-temporal signature of degranulation distinct from that induced following FcγR-crosslinking. Non-sensitized PBCMCs were stimulated with 2 μg/ml of C5a (purple), 2 μg/ml of C3a (cyan), 1 μM of ET-1 (gold) or 1 μg/ml of mouse IgG immune complexes (green), in the presence of Av.SRho. Av.SRho fluorescence was measured at the single cell level using time-lapse confocal microscopy in a controlled atmosphere (37ºC and 5% CO_2). (**A**) Percentage of Av.SRho$^+$ cells per field as compared to cells stimulated with anti-IgE (blue) or SP (pink). (**B**) Av.SRho MFI per single cell as compared to anti-IgE (blue) or SP (pink). (**C**, **E**, **G**, **I**) Representative time-lapse sequence of Av.SRho enrichment (color scale) in single PBCMCs stimulated with (**C**) 2 μg/ml of C5a, (**E**) 2 μg/ml of C3a, (**G**) 1 μM ET-1, and (**I**) 1 μg/ml of mouse IgG immune complexes. (**D**, **F**, **H**, **J**) Curves of single cell analyzes of Av.SRho MFI in PBCMCs stimulated with (**D**) 2 μg/ml of C5a, (**F**) 2 μg/ml of C3a, (**H**) 1 μM of ET-1, and (**J**) 1 μg/ml of mouse IgG immune complexes (in each graph, the same data for PBCMCs stimulated with medium alone are presented in grey color for reference). (**K**) Mean ± SEM of pooled experiments described in **D**, **F**, **H**, **J**. Bars in **C**, **E**, **G**, **I** = 5 μm. Data in **D**, **F**, **H**, **J**, **K** are from 4 independent experiments performed with cells from 1 donor (between 30 and 40 single PBCMCs analyzed per condition), with replicate experiments giving similar results.

Supplemental Figure 6

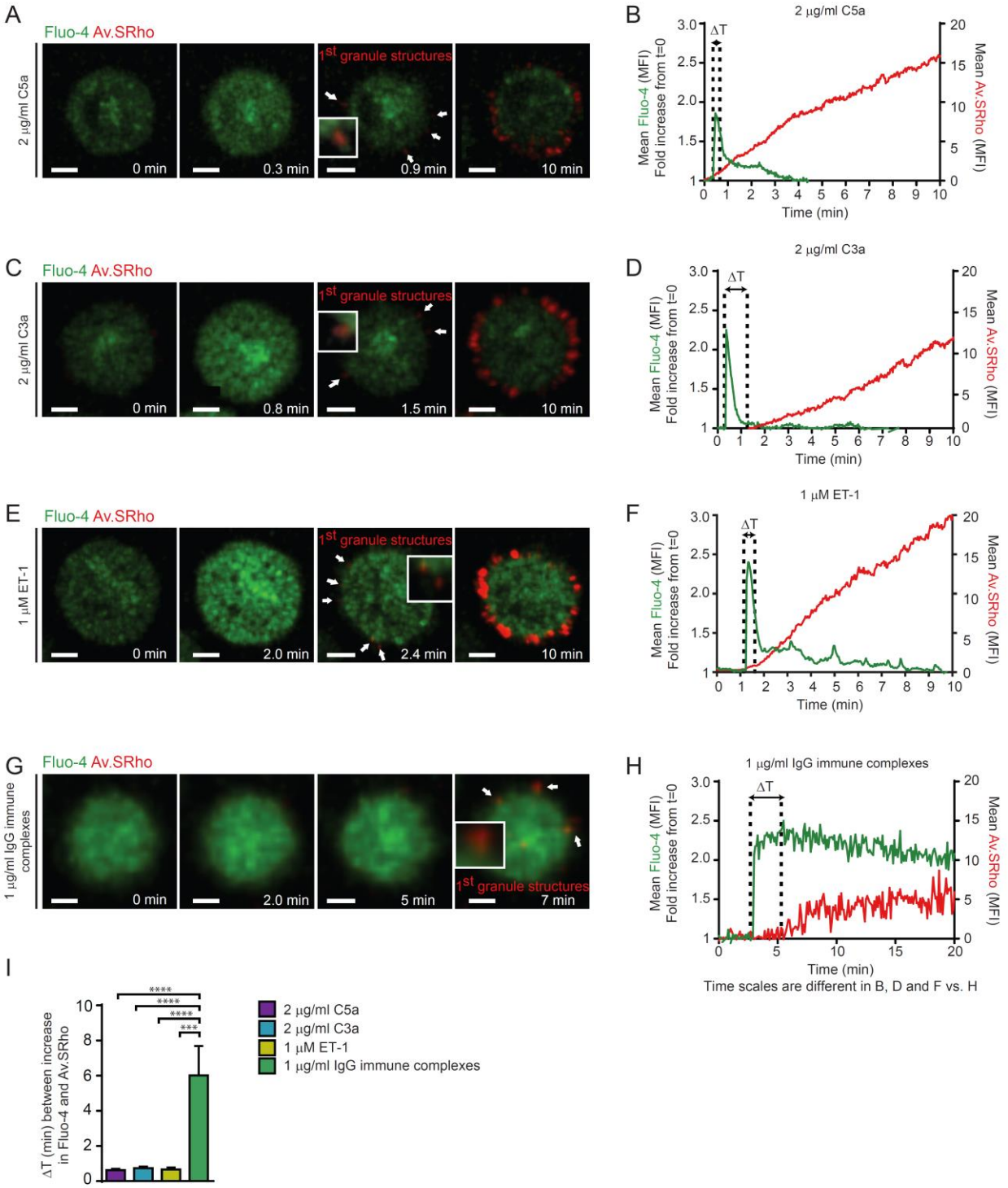

Supplemental Figure 6. Human mast cell activation by C3a, C5a or ET-1 induces a shorter lag time between signaling and secretion than that induced following FcγR-crosslinking.

Non-sensitized Fluo-4-loaded PBCMCs were stimulated with 2 μg/ml of C5a (purple), 2 μg/ml of C3a (cyan), 1 μM of ET-1 (gold) or 1 μg/ml of mouse IgG immune complexes (green), in the presence of Av.SRho. Fluo-4 (green, $[Ca^{2+}]_i$) and Av.SRho (red) fluorescence was measured, at the single cell level, using time-lapse confocal microscopy in a controlled atmosphere (37°C and 5% CO_2). (**A**, **C**, **E**, **G**) Representative time-lapse sequence of a single PBCMC activated with 2 μg/ml of C5a (**A**), 2 μg/ml of C3a (**C**), 1 μM of ET-1 (**E**) or 1 μg/ml of mouse IgG immune complexes (**G**). Bars = 5 μm, white insets show a budding granule structure at higher magnification, arrows indicate first budding granule structures; note that the time sequences of the pictures shown are varied according to the type of stimulation that was assessed. (**B**, **D**, **F**, **H**) Mean curves of Fluo-4 and Av.SRho MFI following stimulation with 2 μg/ml of C5a (**B**), 2 μg/ml of C3a (**D**), 1 μM of ET-1 (**F**) or 1 μg/ml of mouse IgG immune complexes (**H**); dotted lines and arrows indicate the lag time (ΔT) measured between the beginning of the increase in [Ca2+]i and the detection of the first budding granule structures. (**I**) Mean ΔT measured following each type of stimulation. Mean + SEM; two-tailed, unpaired *t* test, ***P < .001, ****P < .0001. Data are from 3 independent experiments performed with PBCMCs from 2 donors (at least 30 single PBCMCs analyzed per condition), each of which gave similar results.

Supplemental Figure 7

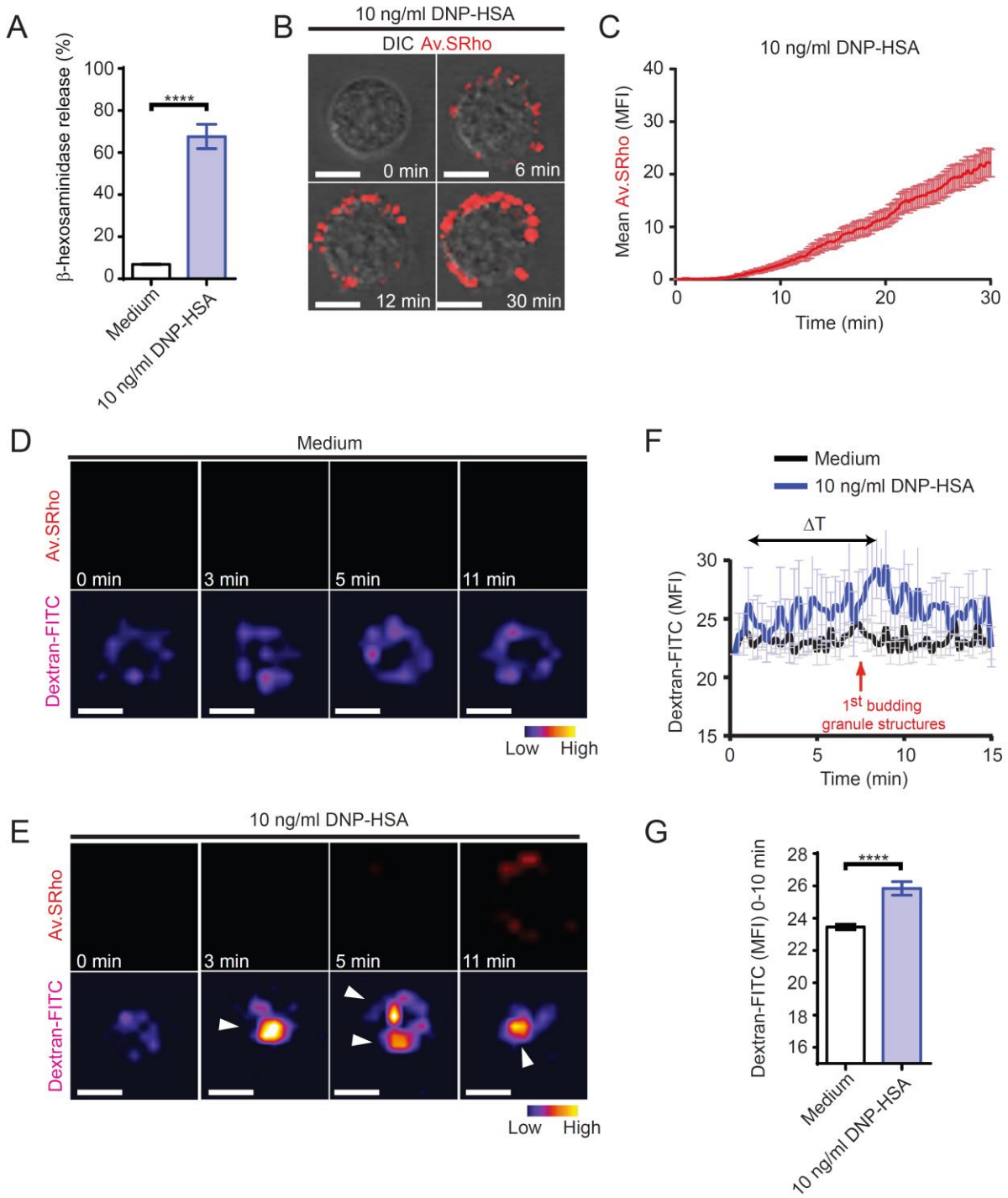

Supplemental Figure 7. Mouse peritoneal cell-derived mast cells (PCMCs) activated *via* IgE and specific antigen exhibit an "anti-IgE-like" degranulation pattern. Anti-DNP IgE-

sensitized PCMCs were stimulated with 10 ng/ml DNP-HSA or vehicle as a control. (**A**) Percentage of β-hexosaminidase release 60 minutes after stimulation. (**B**) Representative time-lapse sequence of a single stimulated PCMC in the presence of Av.SRho (red), fluorescence was measured, at the single cell level, using time-lapse confocal microscopy in a controlled atmosphere (37°C and 5% CO_2). (**C**) Mean curves of pooled single cell analyzes of Av.SRho MFI. (**D**-**G**) Anti-DNP IgE-sensitized dextran-FITC-loaded PCMCs were stimulated with 10 ng/ml DNP-HSA or vehicle (as a control) in the presence of Av.SRho. Dextran-FITC and Av.SRho fluorescence were measured simultaneously, at the single cell level, using time-lapse confocal microscopy in a controlled atmosphere (37°C and 5% CO_2). (**D**) Representative time-lapse sequence of Av.SRho (upper panel, red) and dextran-FITC enrichment (lower panel, pseudo-color scale) in a single PCMC stimulated with vehicle (control) (**D**) or DNP-HSA (**E**). (**F**) Mean curves of pooled single cell analyzes of dextran-FITC MFI in PBCMCs stimulated with vehicle (control, black) or DNP-HSA (blue). (**G**) Average of dextran-FITC MFI between t=0 and t=5 min. Mean ± SEM; two-tailed, unpaired *t* test, ***P<.001; data are from 4 independent experiments (at least 40 single PCMCs analyzed per condition), each of which gave similar results.

Supplemental Figure 8

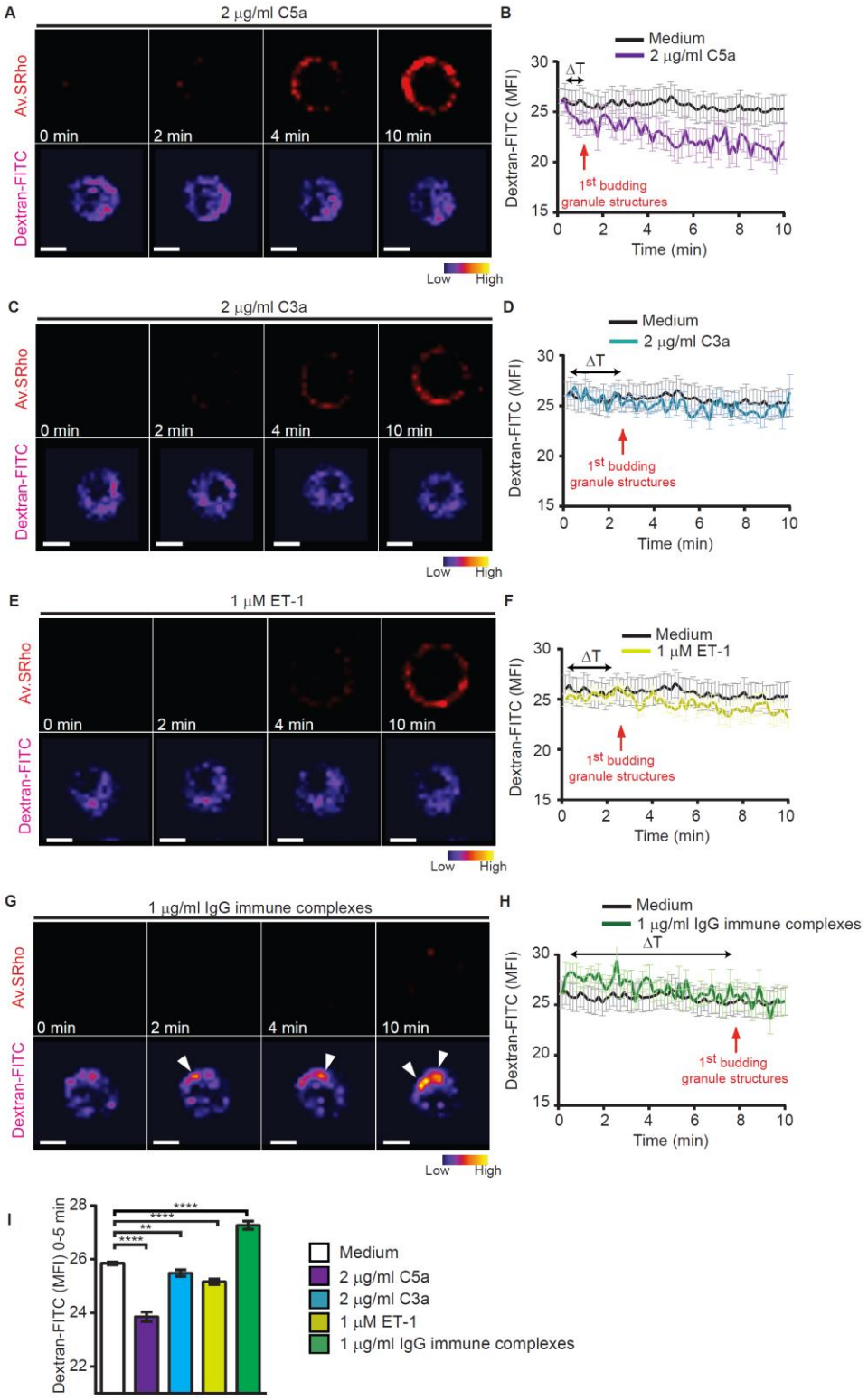

565

Supplemental Figure 8. Human mast cell activation by antibody-independent signals does not enhance intracellular homotypic (i.e., granule-granule) fusion events. PBCMCs were incubated with 1 mg/ml of dextran-FITC for 48 h. PBCMCs not sensitized with IgE were stimulated with 2 μg/ml of C5a (purple) or medium alone (black), in the presence of Av.SRho. Dextran-FITC and Av.SRho fluorescence were measured simultaneously, at the single cell level, using time-lapse confocal microscopy in a controlled atmosphere (37°C and 5% CO_2). (**A**) Representative time-lapse sequence of Av.SRho (upper panel, red) and dextran-FITC enrichment (lower panel, pseudo-color scale) in a single PBCMC stimulated with 2 μg/ml of C5a. (**B**) Mean curve of pooled single cell analyzes of dextran-FITC MFI in PBCMCs stimulated with 2 μg/ml of C5a. (**C**-**H**) Same experiments as the one depicted in (**A**, **B**) but in PBCMCs stimulated respectively with (**C**, **D**) 1 μM of C3a (cyan), (**E**, **F**) 2 μg/ml of ET-1 (gold) or (**G**, **H**) 1 μg/ml of mouse IgG immune complexes (green, white arrows indicate increases in dextran-FITC fluorescence) or medium control (in each graph in **B**, **D**, **F**, **H**, the same data for PBCMCs stimulated with medium alone are presented in a grey color for reference). Bars = 5 μm. The same PBCMCs stimulated with medium alone are used as control in Figure 3 and in Supplemental Figure 8. (**I**) Average of dextran-FITC MFI between t=0 and t=5 min. Mean ± SEM; two-tailed, unpaired *t* test, *P<.05, **P<.01, ****P<.0001; data are from 4 independent experiments performed with PBCMCs from 2 donors (between 30 and 35 single PBCMCs analyzed per condition), each of which gave similar results.

Supplemental Figure 9

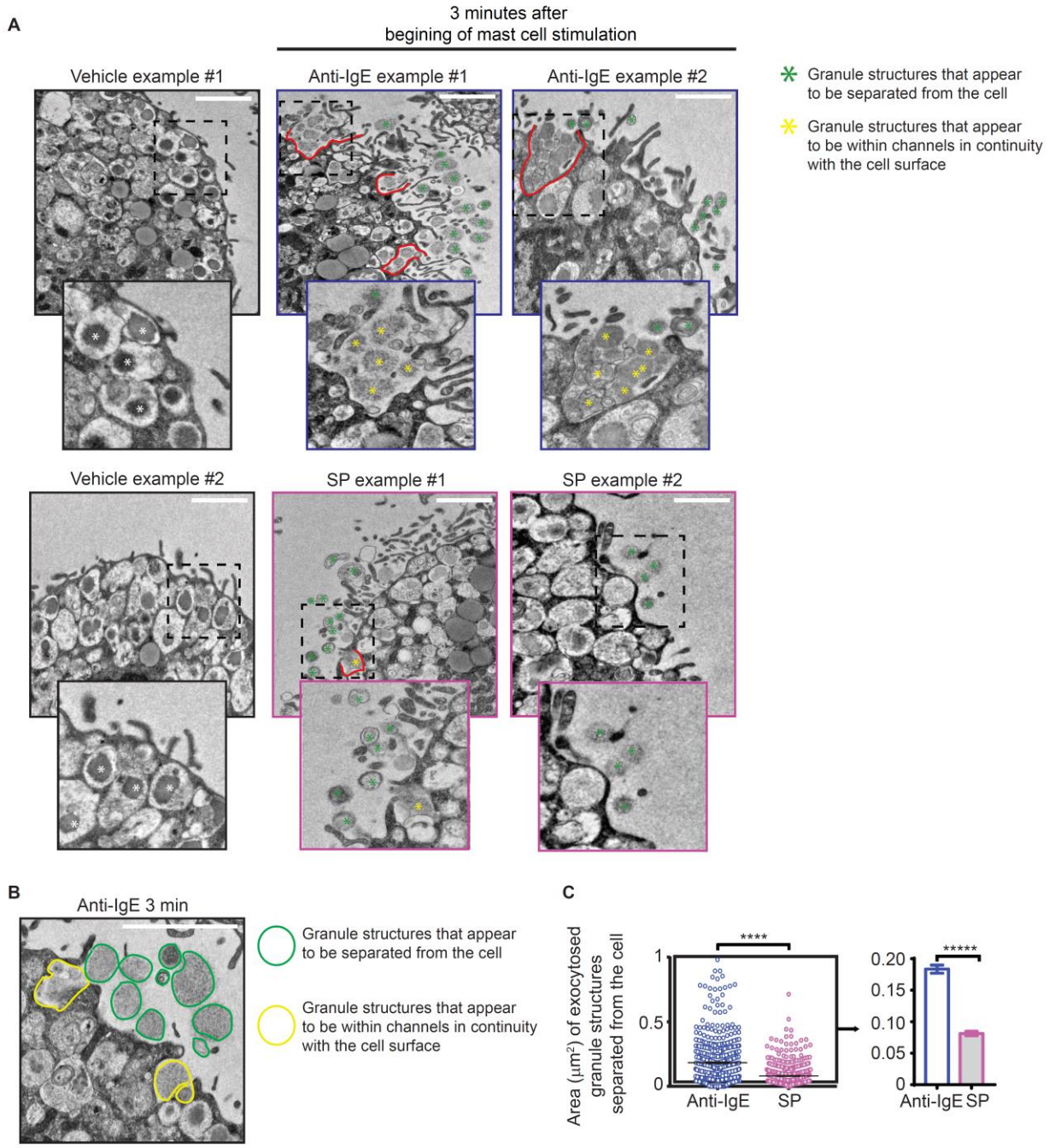

Supplemental Figure 9. TEM analysis of mast cell granule structures exteriorized during Substance P- or anti-IgE-mediated mast cell degranulation. IgE-sensitized or non-sensitized PBCMCs were incubated in the presence of anti-IgE (blue) or SP (pink) respectively, or with RPMI medium alone (No stimulation, black), and analyzed by TEM 3 min after the beginning of

stimulation. (**A**) Representative TEM micrographs of individual PBCMCs; red lines indicate structures ("channels") formed by the fusion of granule membranes with each other and the plasma membrane, green asterisks indicate examples of exteriorized granule structures that are apparently separated from cell, yellow asterisks indicate examples of granule structures that appear to be within channels in continuity with the cell surface, and white asterisks (in cells incubated solely with vehicle) indicate some of the intracellular granule structures. (**B**) Representative high magnification TEM micrograph of a PBCMC stimulated with anti-IgE; green lines indicate examples of the granule structures separated from cell that are analyzed in **panel C**, yellow lines indicate examples of granule structures that appear to be within channels or invaginations in continuity with the cell surface (such granule structures are not included in the data shown in **panel C**). Insets show higher magnifications of the areas indicated with black dotted squares. (**C**) Mean calculated area (in μm^2) of more that ~ 700 individual granule structures visually separated from cell. Left panel: each dot represents one individual granule structure analyzed and right panel: mean ± SEM of the data shown in the left panel. Two-tailed, unpaired *t* test, ****P < .0001. Data are from TEM micrograph of ~ 60 individual PBCMCs per condition from 2 individual experiments performed with 2 donors, each of which gave similar results. Bar = 2 μm.

Supplemental Figure 10

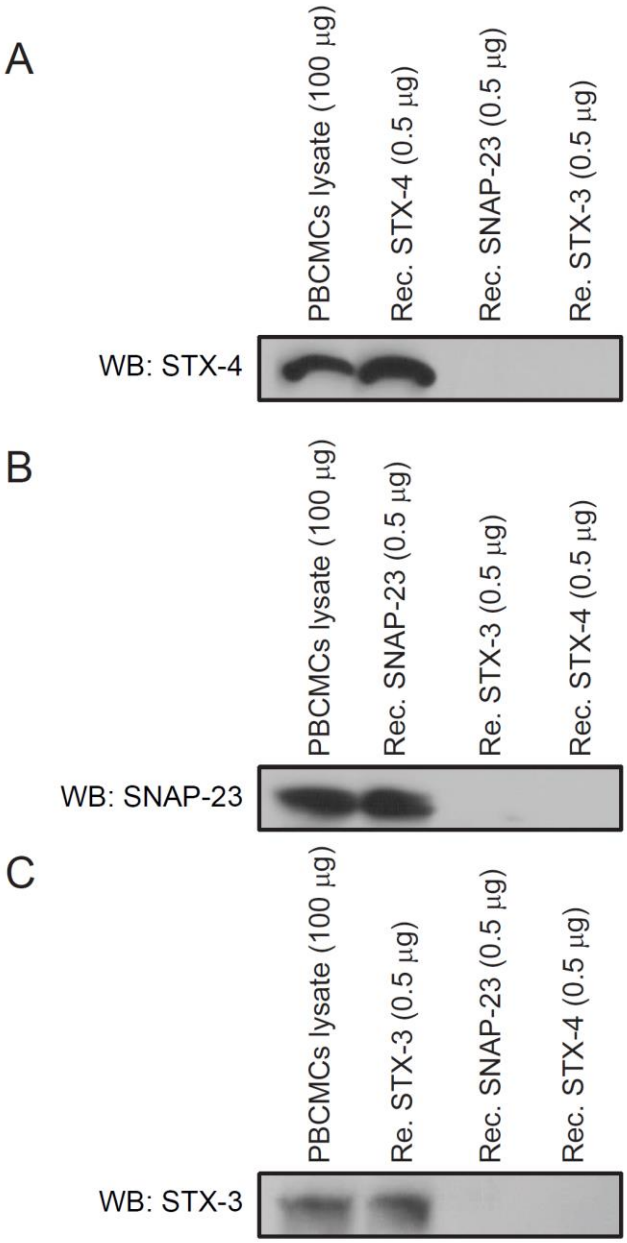

Supplementary Figure 10. Assessment of the specificity of the anti-STX4, anti-SNAP-23 and anti-STX-3 antibodies used for immunoprecipitation. Detection of STX-4 (**A**), SNAP-23 (**B**) or STX-3 (**C**) in lysates of unstimulated PBMCs lysates or in specimens of recombinant human proteins. Data are from 2 independent experiments, each of them performed with PBCMCs from a different single donor, each of which gave similar results.

Supplemental Figure 11

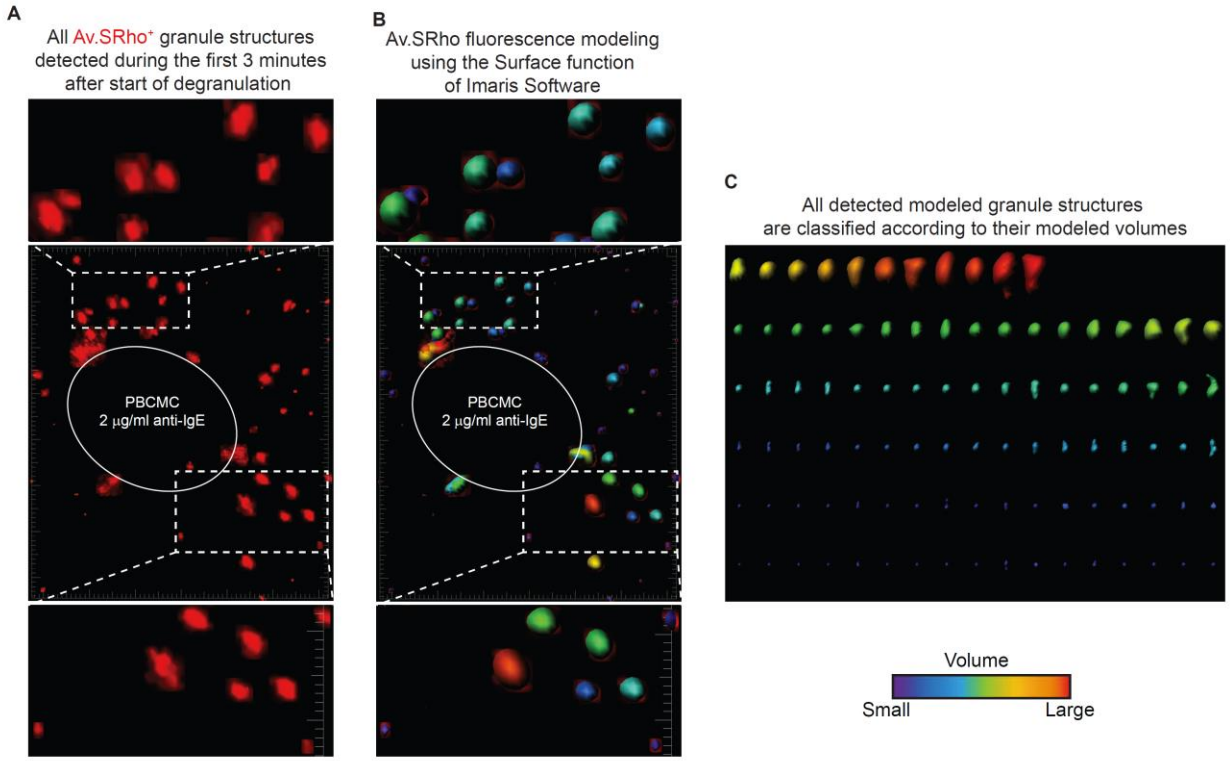

Supplemental Figure 11. Detection and modeling of exteriorized mast cell granule structures using the Av.SRho technique and Surface functions of Imaris. (**A**) Superimposition on the same image of all the Av.SRho$^+$ exteriorized granule structures (which could be individual granules or aggregates of individual granules) detected using confocal laser-scanning microscopy during the first 3 minutes after the beginning of degranulation induced in human PBCMCs stimulated with anti-IgE (conditions as described in Figure 2). This representative picture shows how many Av.SRho$^+$ granule structures are detected in one focal plane during 3 minutes of degranulation. (**B**) Each individual Av.SRho$^+$ granule structure is modeled and converted into a 3-D object; the software takes into consideration the precise shape and intensity of the fluorescent signal. This representative picture shows that most (if not 100%) of the structures with a detectable fluorescent signal are converted into 3-D objects and can be directly analyzed for their modeled volume using a pseudo color intensity scale. (**C**) Classification

of all the created 3-D objects according to their modeled volumes. This picture shows that, in general, the larger of the modeled Av.SRho$^+$ structures have a higher proportion of structures with more irregular shapes.

Supplemental Figure 12

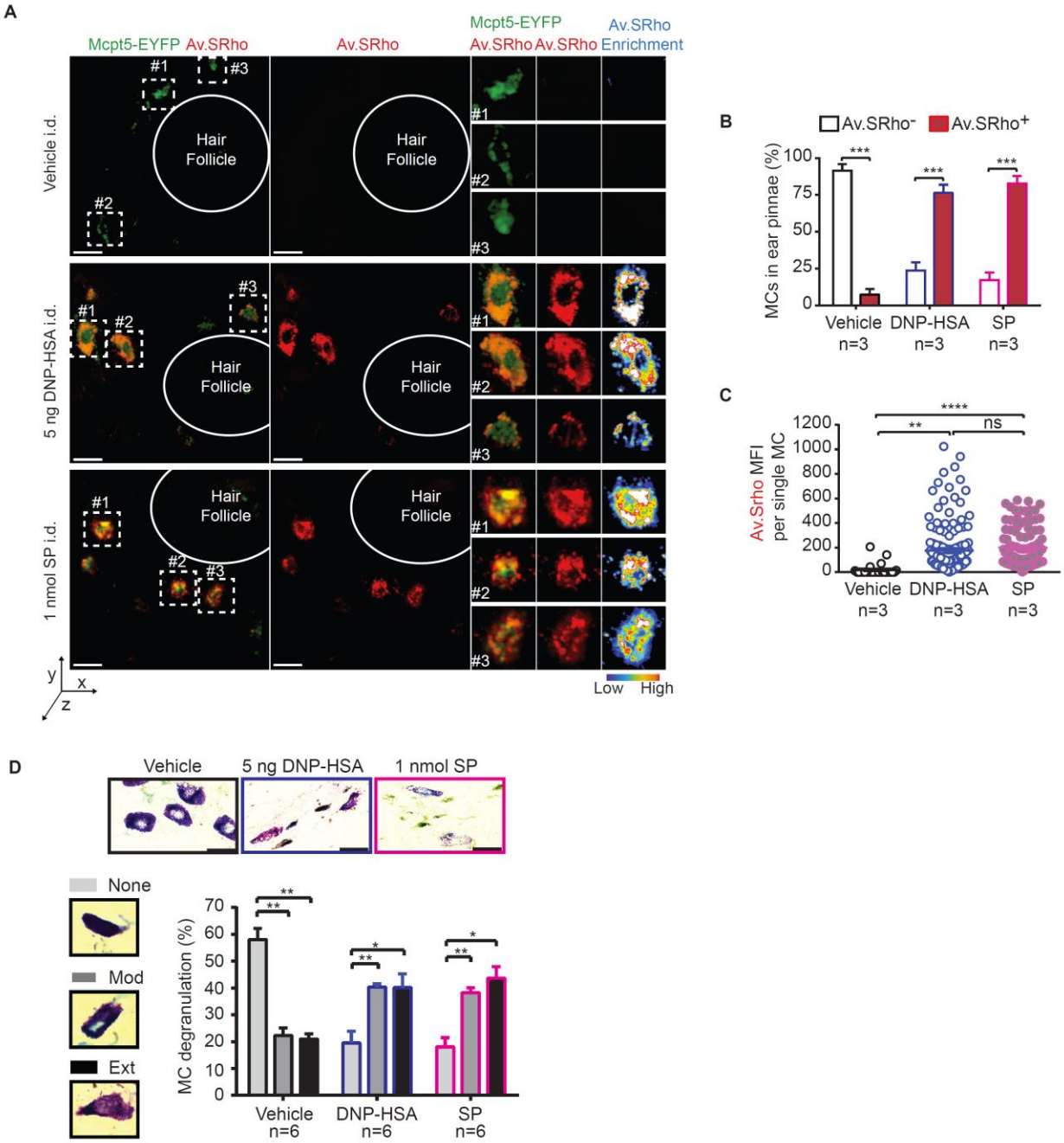

Supplemental Figure 12. I.d injection of 1 nmol of SP or 5 ng of DNP-HSA induces a similar extent of dermal mast cell degranulation. Mice were sensitized by i.d. injection of 20 ng anti-

DNP-HSA IgE into the left ear pinna and vehicle alone (as a control) was injected i.d. into the right ear pinna. 16 h later, the right ear pinna was injected i.d. with 1 nmol of SP (pink) and the left with 5 ng of DNP-HSA (blue). In control experiments, both ear pinnae were injected i.d. with vehicle (black). (**A**) Representative photographs of MC degranulation in the ear pinnae of Mcpt5-EYFP mice 30-60 min after injection of vehicle (upper panels), DNP-HSA (middle panels) or SP (lower panels). From left to right: Av.SRho (red) and EYFP (green) fluorescence merged; Av.SRho (red); 3 examples of degranulated MCs (left to right: Av.SRho/EYFP/Av.SRho/Av.SRho enrichment). Bars = 20 μm. (**B**) Quantification of the percentage of Av.SRho$^+$ (red) vs Av.SRho$^-$ (white) EYFP$^+$ tissue MCs. (**C**) Single cell analysis of Av.SRho MFI (each dot = value for a single MC). (**D**) Toluidine blue analysis of MC degranulation 60 min after injection of vehicle, DNP-HSA or SP; upper panel: representative picture of ear pinnae sections; lower panel: percentage and intensity of MC degranulation, as determined by classification in three categories, not degranulated (None, grey), moderately degranulated (Mod, darker grey) and extensively degranulated (Ext, black). n=total number of mice per condition.

Supplemental Figure 13

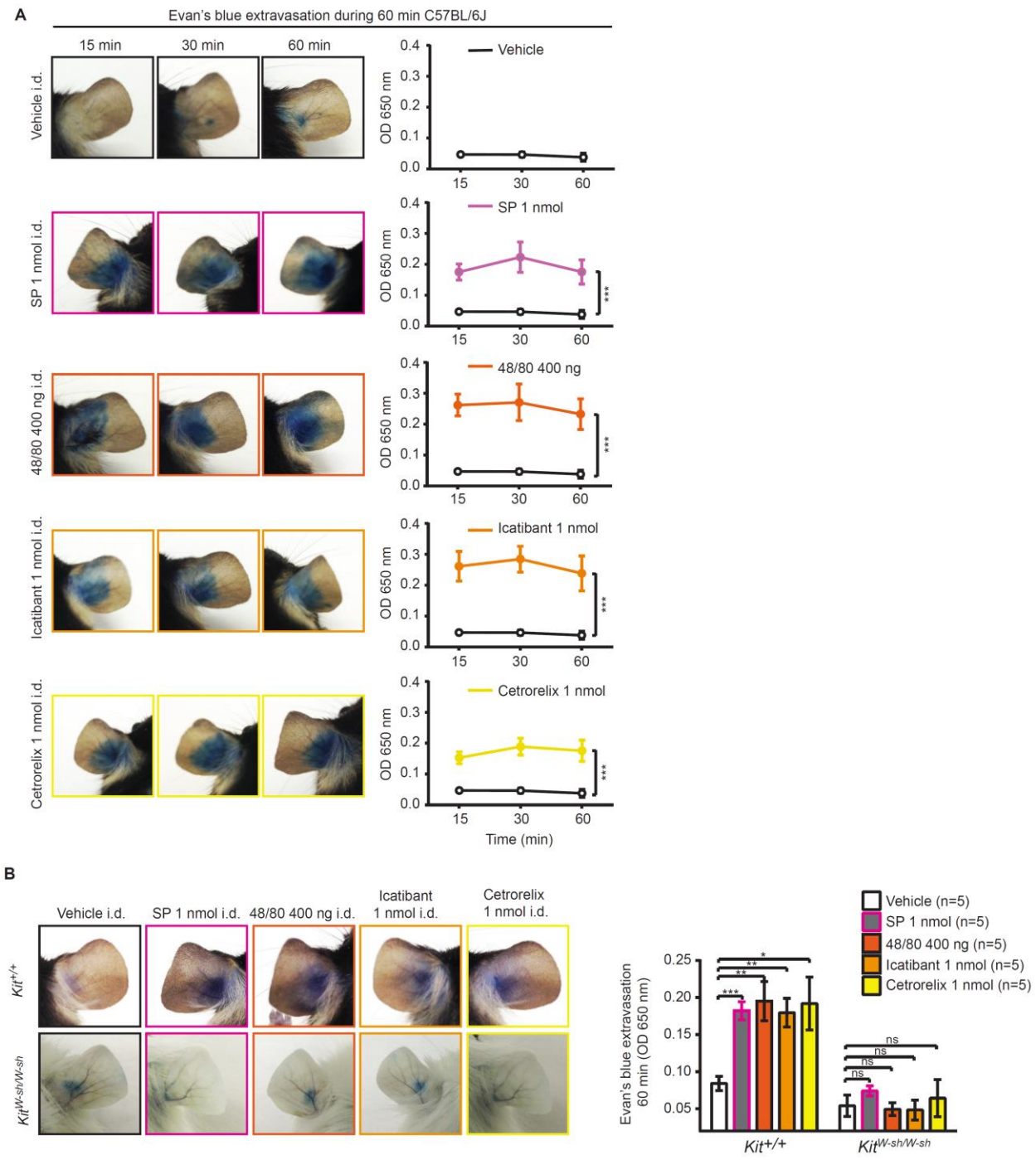

Supplemental Figure 13. Mast cell activation *in vivo* by different cationic compounds results in similar Evan's blue extravasation dynamics. Ear pinnae of naïve mice were injected i.d. with 1 nmol of SP (pink), 400 ng of compound 48/80 (brown), 1 nmol of Icatibant (orange), 1

nmol of Cetrorelix (yellow), or vehicle alone (black). (**A**) Evan's blue extravasation in the ear pinnae of C57BL/6 wild type mice. Left panels: representative photographs of ears, right panels: measurements of Evan's blue extravasation per ear (OD 650 nm), at 15, 30 or 60 min after i.d. injection. Mean ± SEM; two-way ANOVA, ***P<.001. Data are pooled from the 3 independent experiments performed, each of which gave similar results. (**B**) Evan's blue extravasation in the ear pinnae of MC-deficient C57BL/6-*Kit*$^{W\text{-}sh/W\text{-}sh}$ mice versus C57BL/6 wild-type mice. Left panels: representative photographs of ears and right panels: measurements of Evan's blue extravasation per ear (OD 650 nm), 60 min after i.d. injection. Mean ± SEM; two-tailed, unpaired *t* test, *P<.05 **P<.01 ***P<.001. Data are pooled from 3 independent experiments performed, each of which gave similar results. n=total number of mice per condition.

Supplemental Figure 14

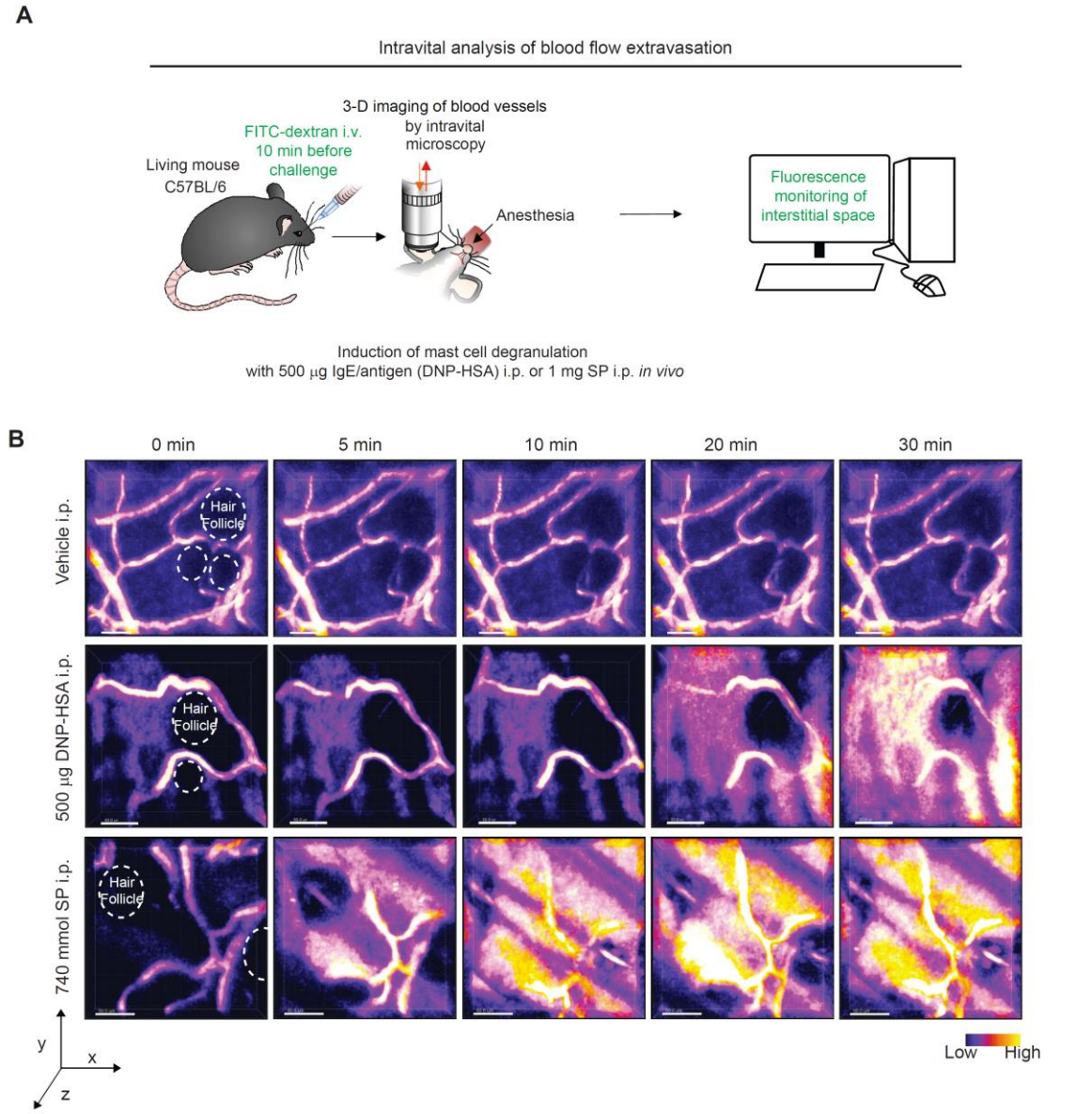

658

Supplemental Figure 14. Different effects on plasma extravasation dynamics and body temperature during MRGPRB2- vs. FcεRI-mediated responses in mice. (**A**) *C57BL/6* wild type mice were sensitized or not with i.d. injection into the ear pinna of 20 ng of mouse anti-DNP-HSA IgE or vehicle as a control. 16 h later, we retro-orbitally injected 250 μg of 70-kDa dextran-FITC and the anesthetized mouse was positioned under the two-photon microscope. Non-sensitized mice were injected i.p. with 1 mg of SP. Anti-DNP IgE-sensitized mice were injected i.p. with 500 μg of DNP-HSA. In control experiments, sensitized mice were injected i.p. with vehicle alone. Image sequences were acquired in 3-D at a rate of one picture per min over 30 min. (**B**) Representative 3-D time-lapse sequences of dextran-FITC fluorescence. Bars = 50 μm. (**C**) Fold changes in dextran-FITC MFI in the interstitial space following injection of SP (pink), DNP-HSA (blue) or vehicle (black). (**D**) C57BL/6-*Kit*$^{+/+}$ or C57BL/6-*Kit*$^{W\text{-}sh/W\text{-}sh}$ mice were sensitized or not with an i.p. injection of 10 μg of mouse anti-DNP-HSA IgE. 16 h later, non-sensitized or sensitized animals were injected i.p. with 1 mg of SP (pink) or 500 μg of DNP-HSA (blue), respectively, or with vehicle alone (black). Mouse body temperature (^{o}C) was measured over 120 min. (**C**-**D**) Mean ± SEM; two-way ANOVA, **P < .01, ***P < .001, ****P < .0001. Data were pooled from the 3 individual experiments performed for each condition of stimulation, each of the replicate experiments giving similar results. n=total number of mice per condition.

Supplemental Video 1. Human mast cell intracellular calcium flux and degranulation dynamics upon stimulation with anti-IgE or SP. IgE-sensitized or non-sensitized PBCMCs were loaded with Fluo-4 and stimulated with anti-IgE antibodies or SP in the presence of Av.SRho. Fluo-4 (green, [Ca2+]i) and Av.SRho (red) fluorescence signals were monitored, at the single cell level, using time-lapse confocal microscopy in a controlled atmosphere (37°C and 5% CO_2).

Supplemental Video 2. Monitoring of dextran-FITC fluorescence dequenching in human mast cells stimulated with anti-IgE or SP. PBCMCs were incubated with 1 mg/ml of dextran-FITC for 48 h. IgE-sensitized or non-sensitized PBCMCs were stimulated with 2 μg/ml of anti-IgE or 10 μM of SP, respectively, or with vehicle alone, in the presence of Av.SRho. Dextran-FITC (pseudo-color scale) and Av.SRho (red) fluorescence signals were monitored, at the single cell level, using time-lapse confocal microscopy in a controlled atmosphere (37ºC and 5% CO_2).

Supplemental Video 3. Monitoring of dextran-FITC fluorescence dequenching in human mast cells stimulated with C5a, C3a, ET-1 or IgG immune complexes. PBCMCs were incubated with 1 mg/ml of dextran-FITC for 48 h. Non-sensitized PBCMCs were stimulated with 1 μg/ml of C5a (purple), 1 μg/ml of C3a (cyan), 1 μM of ET-1 (gold), 1 μg/ml of IgG immune complexes (green), or with vehicle alone (white), in the presence of Av.SRho. Dextran-FITC (pseudo-color scale) and Av.SRho (red) fluorescence were monitored, at the single cell level, using time-lapse confocal microscopy in a controlled atmosphere (37ºC and 5% CO_2).

Supplemental Video 4. Effects of treatment with an IKKβ selective inhibitor on human mast cell intracellular calcium flux and degranulation dynamics. IgE-sensitized or non-sensitized PBCMCs were pretreated during 60 min with 100 μM of BMS-345541 or DMSO as a control, loaded with Fluo-4 and stimulated with anti-IgE antibodies or SP in the presence of Av.SRho. Fluo-4 (green, $[Ca_2^+]i$) and Av.SRho (red) fluorescence signals were monitored, at the single cell level, using time-lapse confocal microscopy in a controlled atmosphere (37ºC and 5% CO_2).

Supplemental Video 5. Effects of treatment with an IKKβ selective inhibitor on dextran-FITC fluorescence dequenching in human mast cells stimulated with anti-IgE. PBCMCs were incubated with 1 mg/ml of dextran-FITC for 48 h. IgE-sensitized or non-sensitized PBCMCs

were pretreated during 60 min with 100 μM of BMS-345541 or DMSO as a control and stimulated with 2 μg/ml of anti-IgE in the presence of Av.SRho. Dextran-FITC (pseudo-color scale) and Av.SRho (red) fluorescence signals were monitored, at the single cell level, using time-lapse confocal microscopy in a controlled atmosphere (37ºC and 5% CO_2).

Supplemental Video 6. Modeling of budding granule structures in human mast cells stimulated with anti-IgE or SP. IgE-sensitized or non-sensitized PBCMCs were stimulated with 2 μg/ml of anti-IgE or 10 μM of SP, respectively, in the presence of Av.SRho (red). Fluorescence was acquired using a confocal microscope and individual budding granule structures (i.e., those undergoing exteriorization and therefore available to bind Av.SRho) were modeled using the Isosurface function of Imaris software. Videos of MCs are started when the first budding granule structures were detected in that cell.

Supplemental Video 7. Modeling of externalized granule structures in human mast cells stimulated with anti-IgE or SP. IgE-sensitized or non-sensitized PBCMCs were loaded with Fluo-4 (green), embedded in a surrogate extracellular matrix gel and stimulated with 2 μg/ml of anti-IgE or 10 μM of SP, respectively, or with vehicle alone, in the presence of Av.SRho (red). 30 min later, 3-D pictures were acquired using a confocal microscope and the fluorescence of granule matrices released beyond the perimeter of the MCs was modeled using the Isosurface function of Imaris software. In the video, the transition from the actual images obtained to modeled fluorescence occurs roughly at the mid-point of the video.

Supplemental Video 8. Analysis of mast cell granule structures exteriorized during IgE-dependent or IgE-independent reactions *in vivo*. *Mcpt5-Cre*$^+$; *R26Y*$^+$ mice were sensitized or not by i.d. injection into the ear pinna of 20 ng of mouse anti-2, 4-dinitrophenyl (DNP) IgE. 16 h

later, 8 μg of Av.SRho was injected i.d. into the same ear pinna. Non-sensitized mice were injected i.p. with 1 mg of SP. Anti-DNP IgE-sensitized mice were injected i.p. with 500 μg of DNP-HSA. In control experiments, IgE-sensitized mice were injected i.p. with vehicle. 30 minute later, 3-D pictures were acquired using a two-photon microscope and fluorescence corresponding to $EYFP^+$ MCs (green) and Av.SRho (red) (identifying budding or exteriorized granule structures) was modeled using the Isosurface function of Imaris software. In the video, the transition from actual obtained images to modeled fluorescence occurs roughly at the mid-point of the video.

Supplemental Video 9. Plasma extravasation dynamics during IgE-dependent or IgE-independent reactions *in vivo*. C57BL/6 wild type mice were sensitized or not by i.d. injection into the ear pinna of 20 ng of mouse anti-DNP IgE or vehicle. 16 h later, we retro-orbitally injected 250 μg of 70-kDa dextran-FITC (pseudo-color scale) and the anesthetized mice were positioned under the two-photon microscope. Non-sensitized mice were injected i.p. with 1 mg of SP and anti-DNP IgE-sensitized mice were injected i.p. with 500 μg of DNP-HSA. In control experiments, IgE-sensitized mice were injected i.p. with vehicle. Image sequences were acquired in 3-D at a rate of one picture per min over 30 min using a two-photon microscope.

Full unedited gel for Figure 3H
Phospho AKT

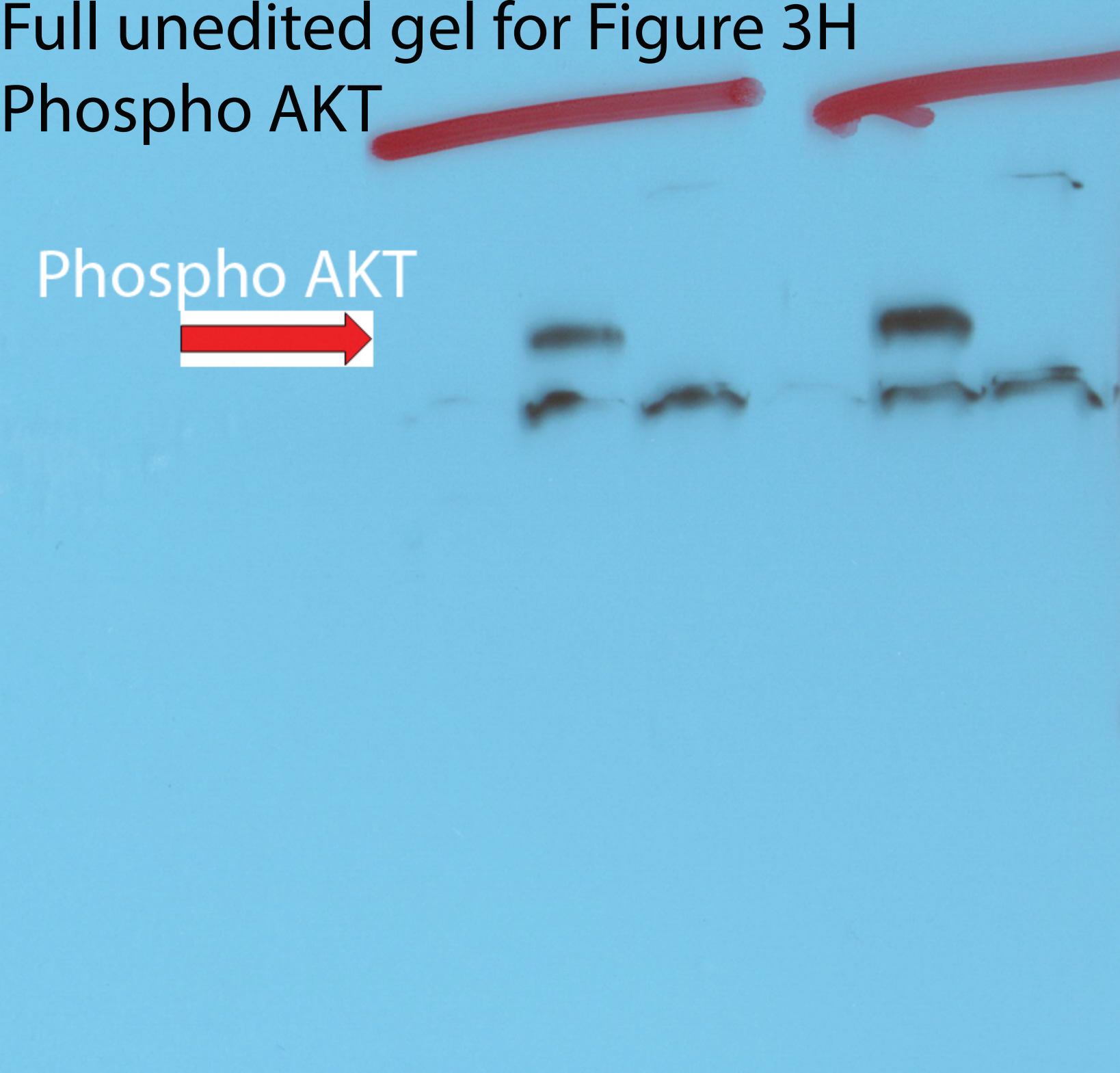

Full unedited gel for Figure 3H Phospho IKKb

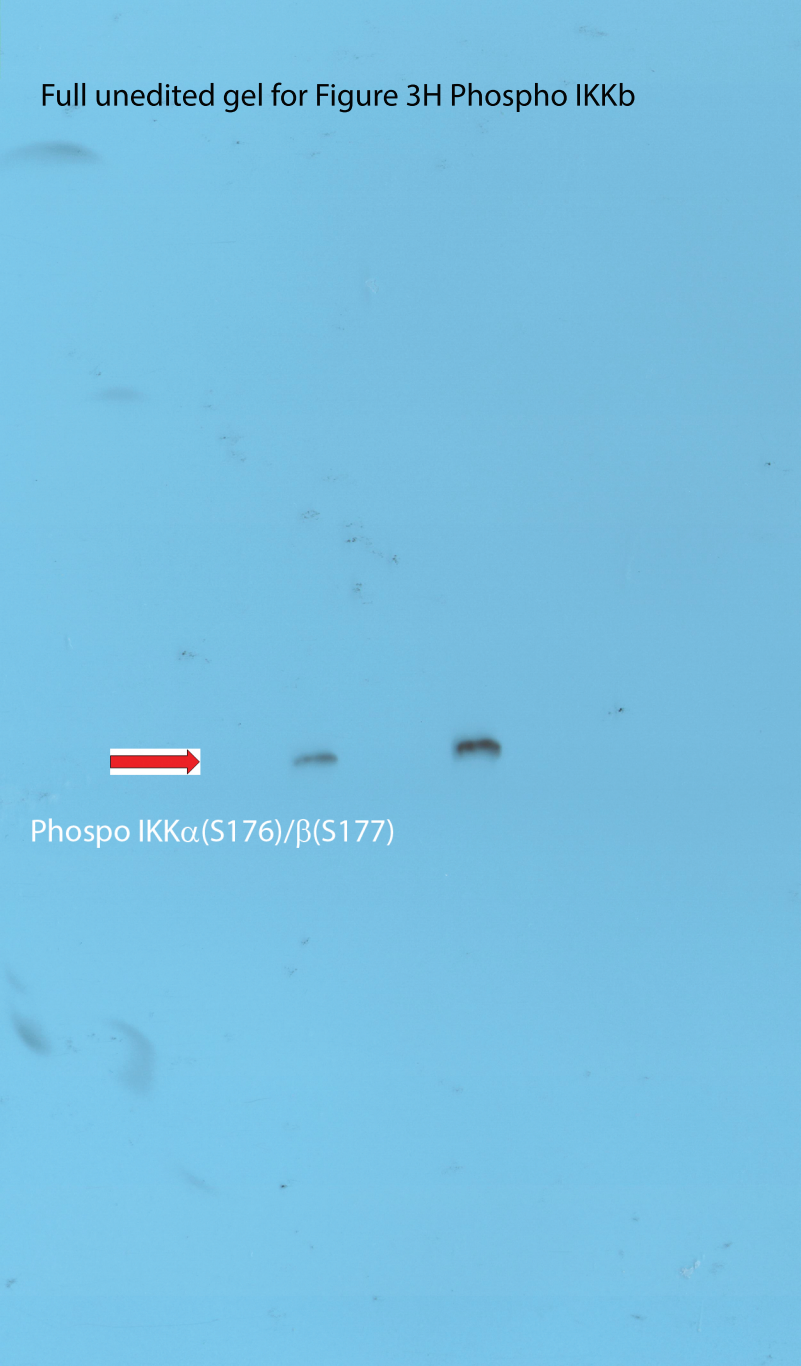

Full unedited gel for Figure 3H Phospho PKC

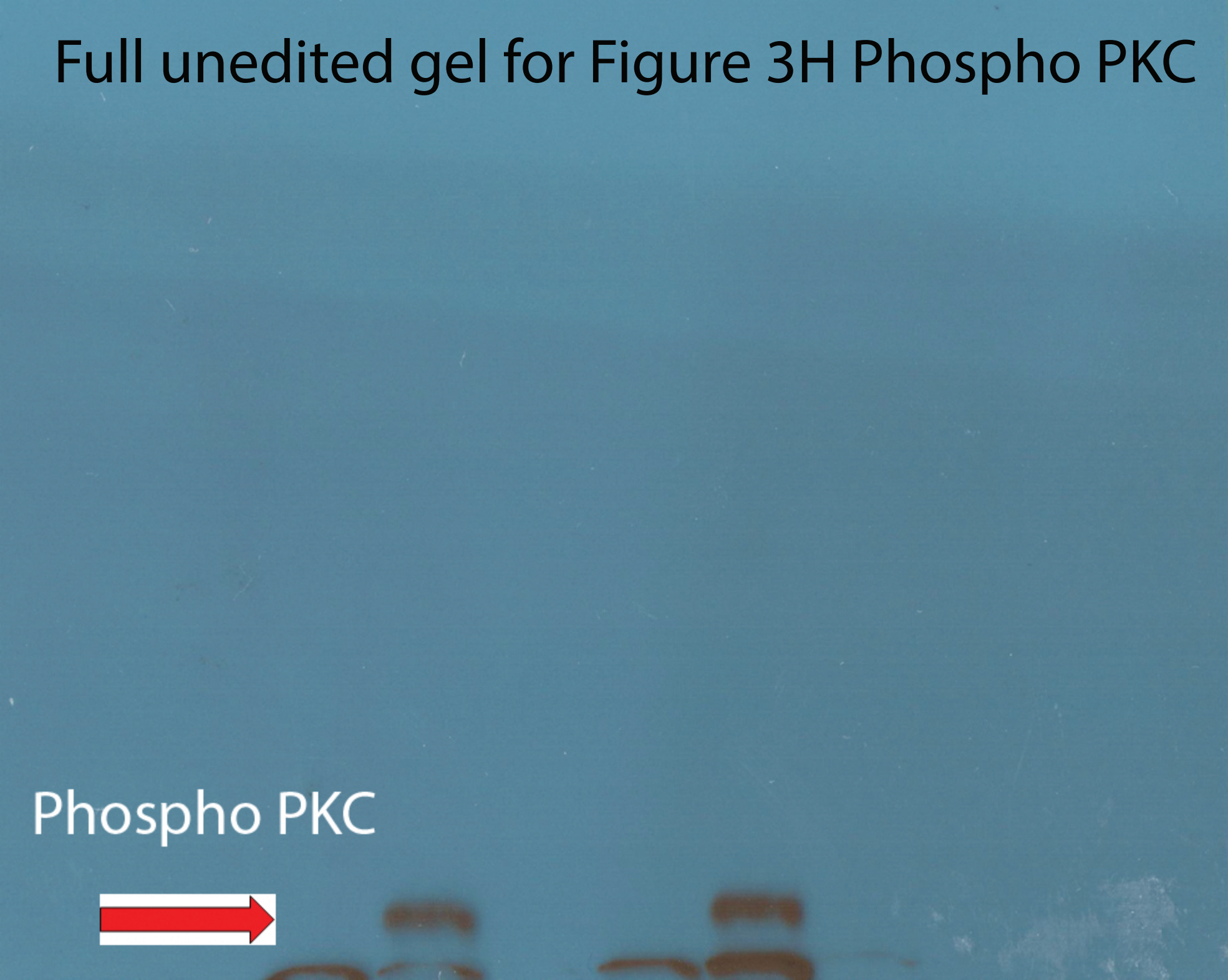

Full unedited gel for Figure 3H total Actin

Full unedited gel for Figure 3I coIP STX4

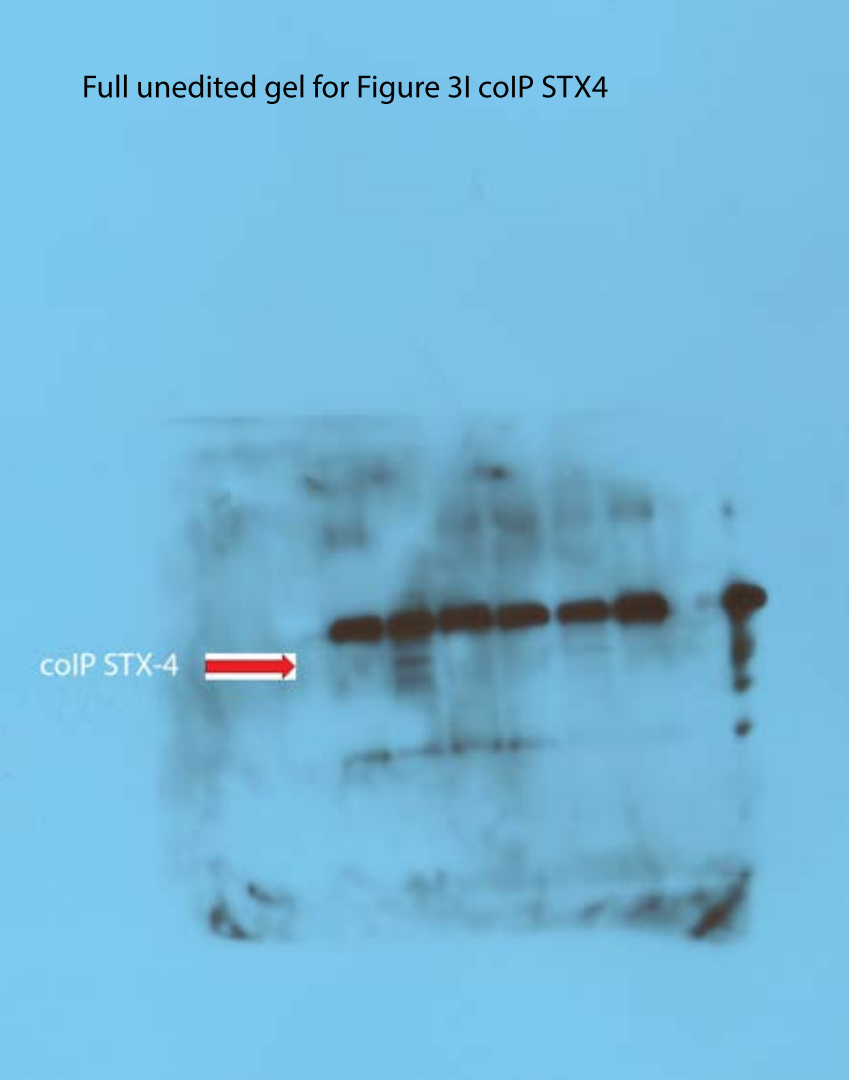

Full unedited gel for Figure 3I IP SNAP23

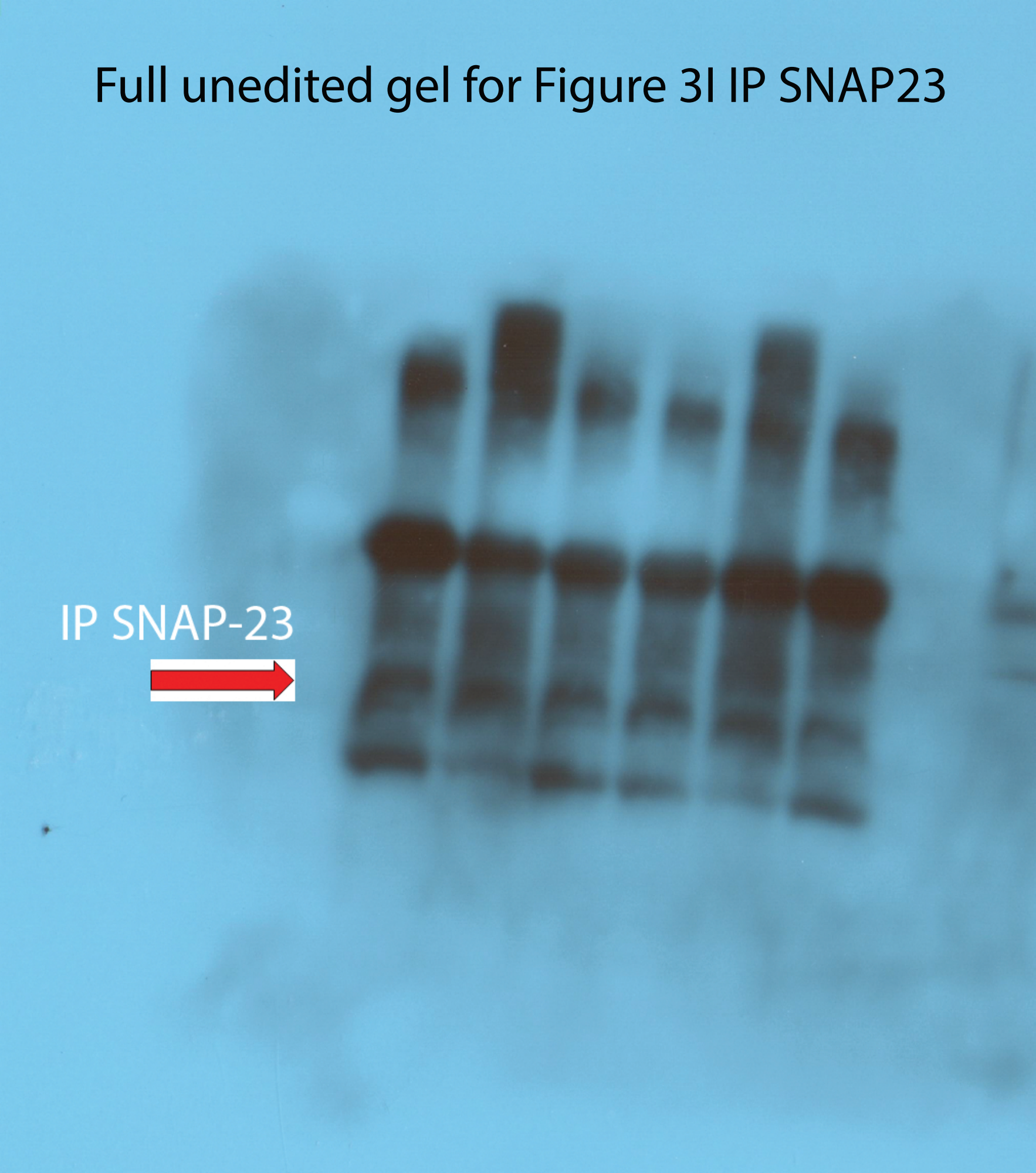

Full unedited gel for Figure 3J coIP STX3

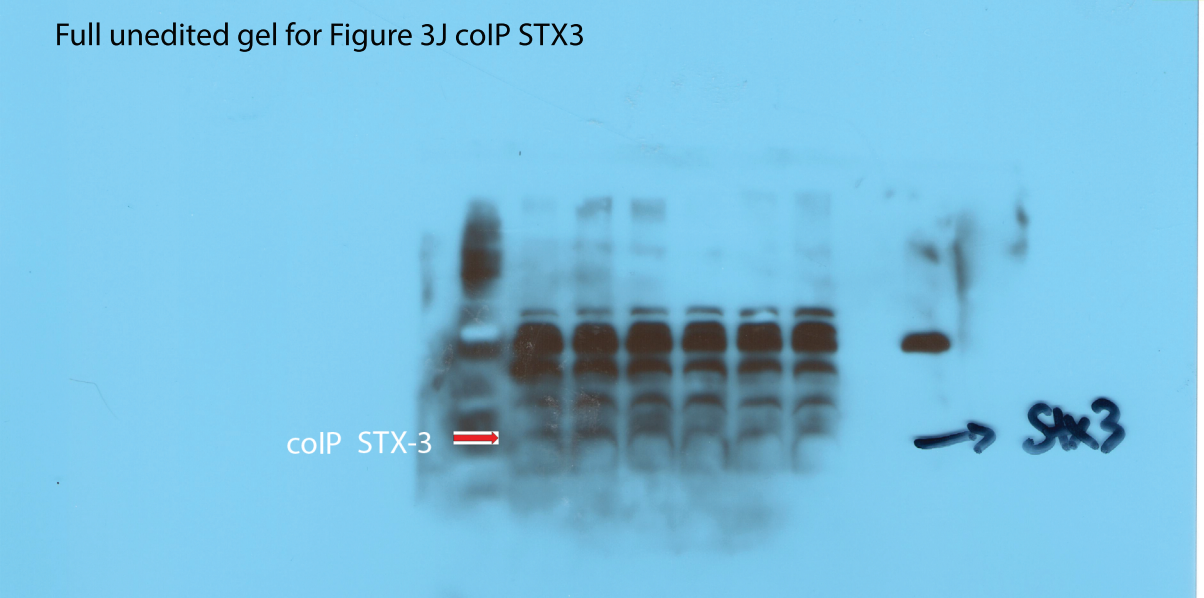

Full unedited gel for Figure 3J IP MUNC18.2

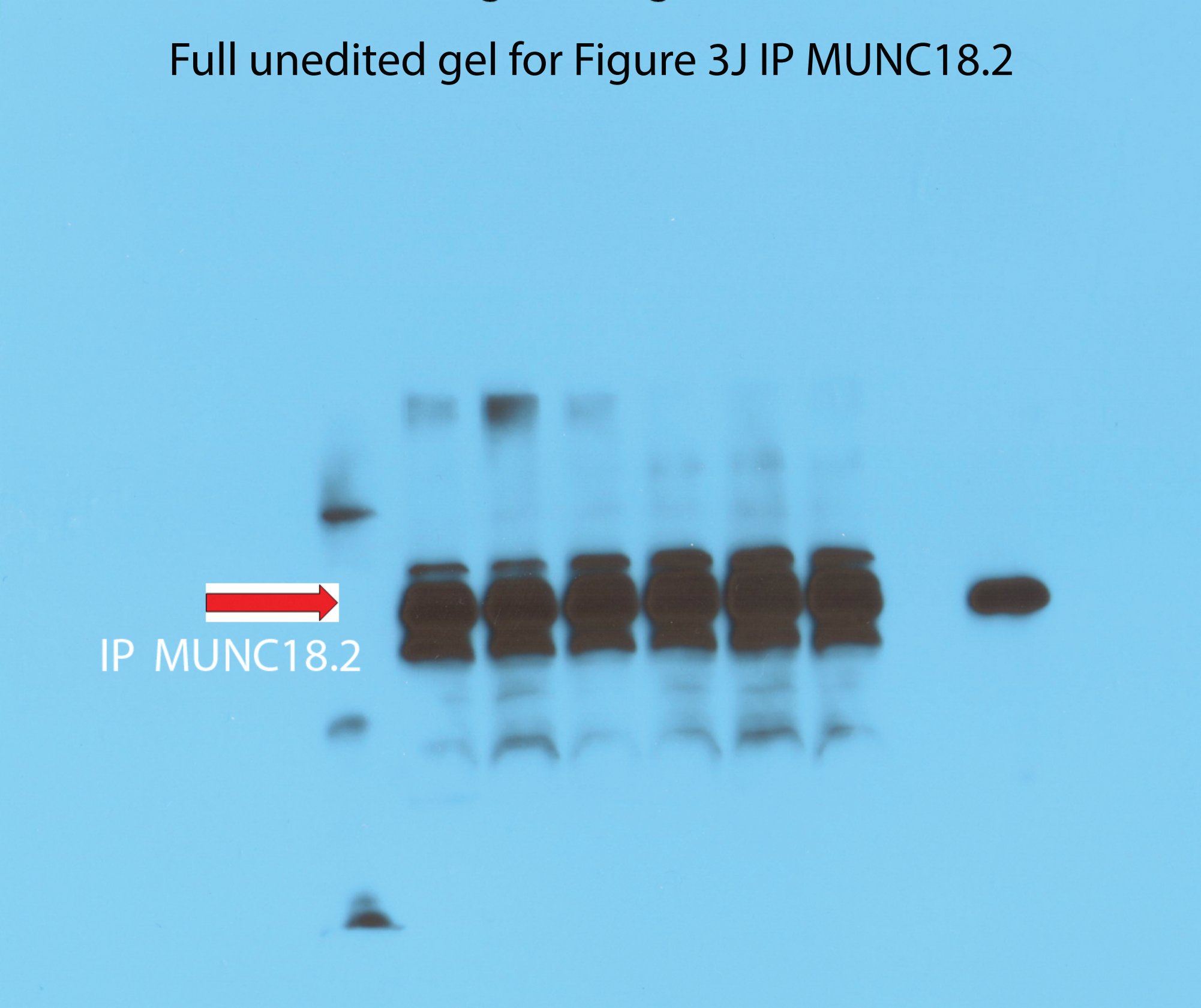

Full unedited gel for Figure 4E Phospho IKKb

Full unedited gel for Figure 4E total Actin

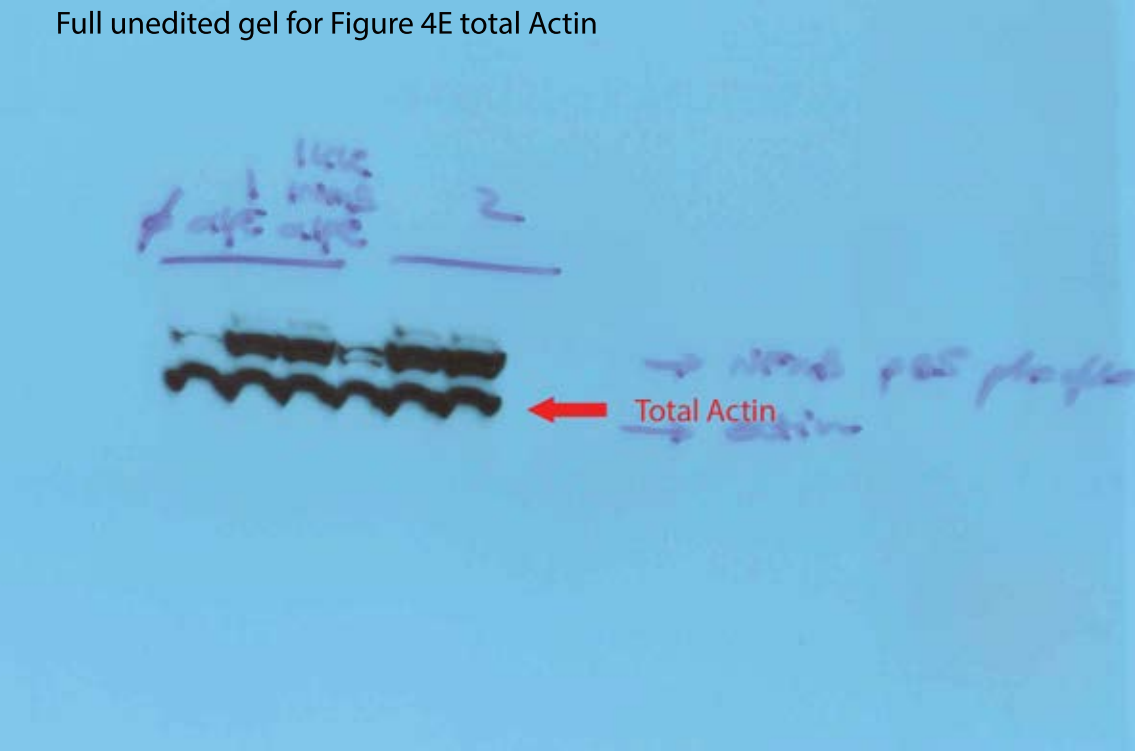

Full unedited gel for Figure 4F coIP STX4

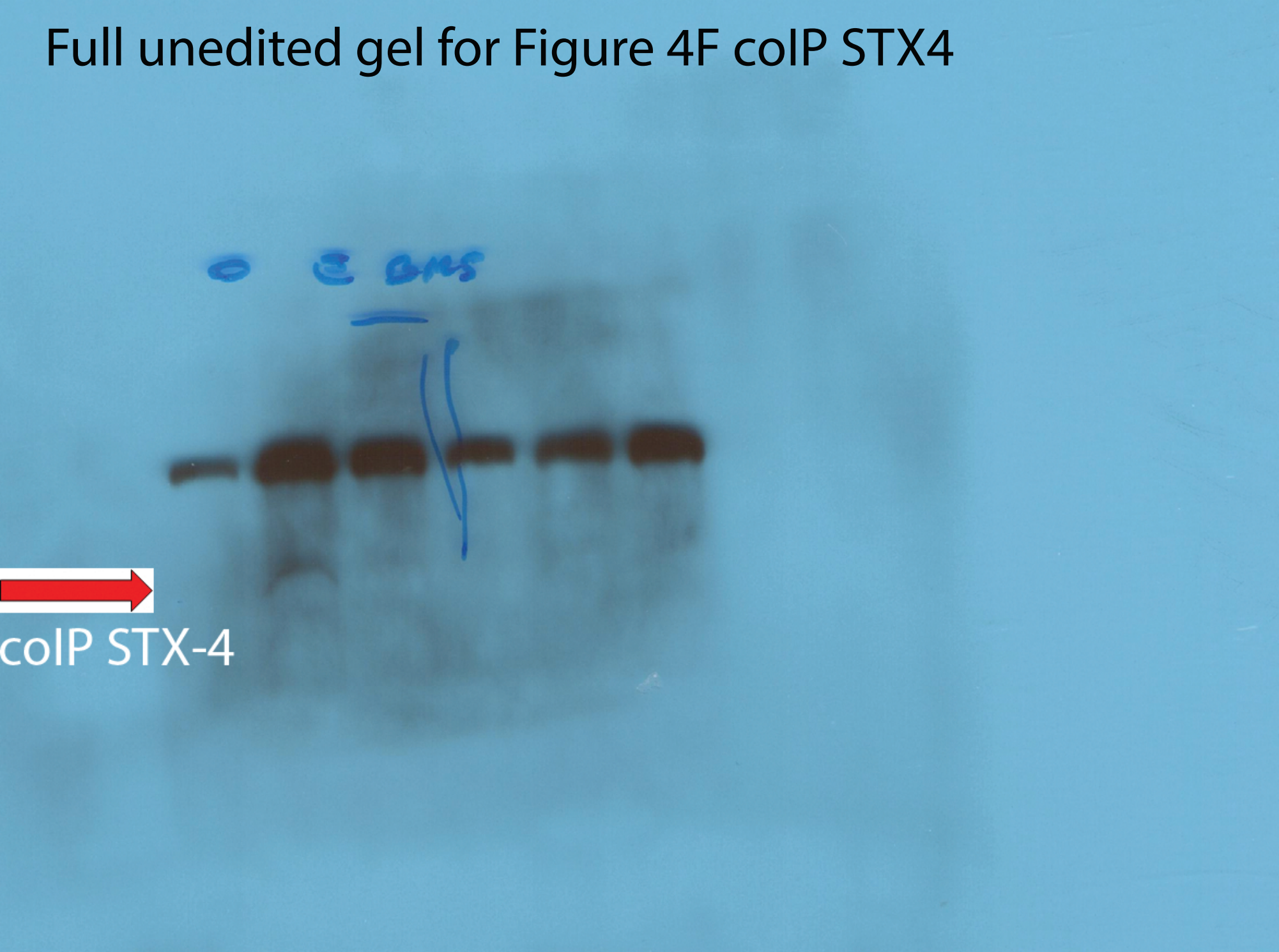

Full unedited gel for Figure 4F IP SNAP23

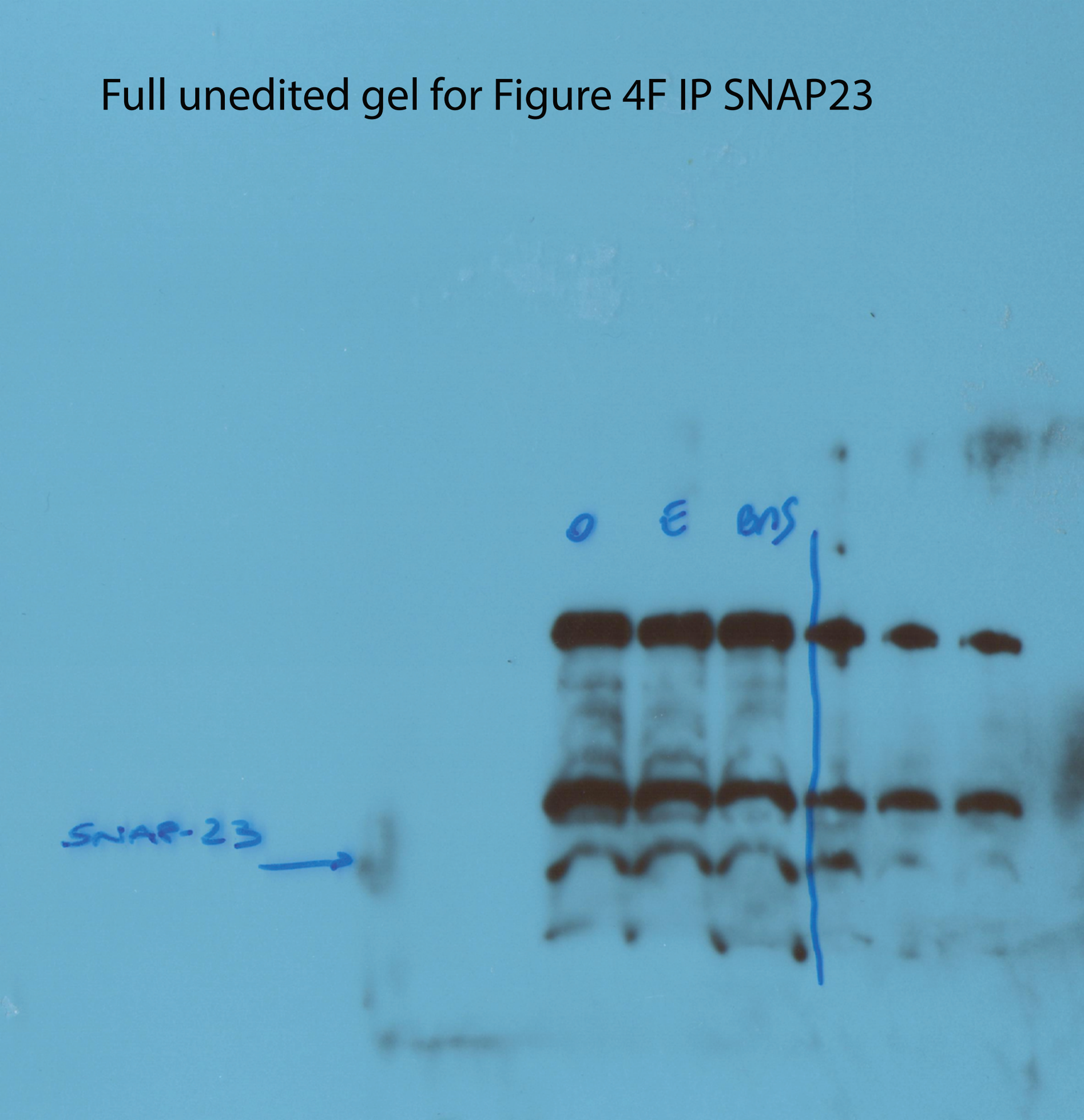

Full unedited gel for Supplemental Figure 10 SNAP23

Full unedited gel for Supplemental Figure 10 STX3

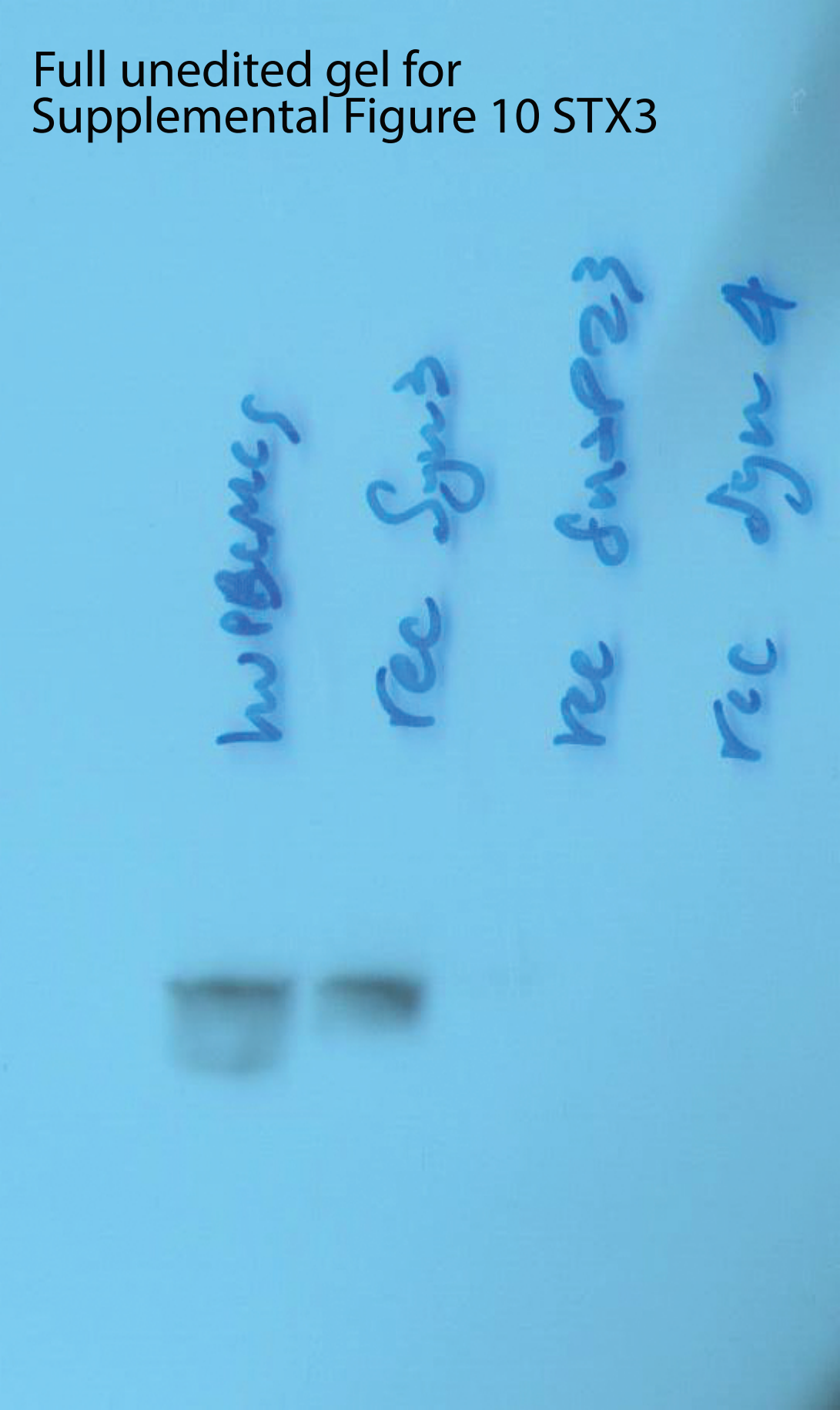

Full unedited gel for Supplemental Figure 10
STX4